Journal Pre-proof

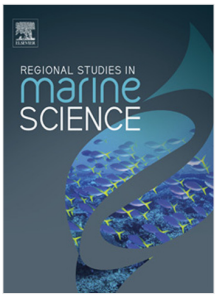

Numerical simulation of Dissolved Oxygen as a water quality indicator in artificial lagoons–Case study El Gouna, Egypt

Omnia Abouelsaad, Elena Matta, Mohie ElDin M. Omar, Reinhard Hinkelmann

PII: S2352-4855(22)00292-4
DOI: https://doi.org/10.1016/j.rsma.2022.102697
Reference: RSMA 102697

To appear in: *Regional Studies in Marine Science*

Received date : 23 November 2021
Revised date : 10 June 2022
Accepted date : 8 October 2022

Please cite this article as: O. Abouelsaad, E. Matta, M.E.M. Omar et al., Numerical simulation of Dissolved Oxygen as a water quality indicator in artificial lagoons–Case study El Gouna, Egypt. *Regional Studies in Marine Science* (2022), doi: https://doi.org/10.1016/j.rsma.2022.102697.

Title: Numerical Simulation of Dissolved Oxygen as A Water Quality Indicator in Artificial Lagoons – Case Study El Gouna, Egypt

Authors: Omnia Abouelsaad[1, 2], Elena Matta[3,1], Mohie ElDin M. Omar [4,5] and Reinhard Hinkelmann[1]

Affiliations:

[1] Technische Universität Berlin, Chair of Water Resources Management and Modeling of Hydrosystems, Germany

[2] Irrigation and Hydraulics Department, Mansoura University, Mansoura city, Egypt

[3] Politecnico di Milano - Department of Electronics, Information, and Bioengineering, Environmental Intelligence Lab, Milano, Italy

[4] National Water Research Center (NWRC), Egypt

[5] International Center of Agriculture Research in the Dry Areas (ICARDA), Egypt

Corresponding author: Omnia Abouelsaad, Technische Universität Berlin, Chair of Water Resources Management and Modeling of Hydrosystems, Gustav-Meyer-Allee 25, 13355 Berlin, Germany. Tel.: +49 30 314 72238

E-mail: o.abouelsaad@campus.tu-berlin.de

NUMERICAL SIMULATION OF DISSOLVED OXYGEN AS A WATER QUALITY INDICATOR IN ARTIFICIAL LAGOONS - CASE STUDY EL GOUNA, EGYPT

Abstract

Dissolved oxygen (DO) is one of the most significant environmental indicators of water quality. Preservation of reasonable DO concentrations is essential for a healthy aquatic life. In this research, numerical simulations of DO concentrations were discussed using TELEMAC-WAQTEL-O_2 model. Firstly, the model was verified by comparing its results to analytical solutions in different 1D and 2D cases considering pulse and constant DO injections. Based on the very good agreement between the model and analytical results in different simulation scenarios, the TELEMAC-WAQTEL-O_2 model has proven its ability to be applied to more complex cases. Consequently, this model was applied to investigate El Gouna artificial lagoons in Egypt under the effect of different weather conditions including tide, mean and maximum wind and different water temperatures. Investigating the water quality of El Gouna lagoons is important to monitor negative anthropogenic impacts to protect the lagoons and the nearby Red Sea coast. Negative effects of effluents from a nearby desalination plant on DO concentration were discussed considering different brine discharges, DO concentrations of brine discharge, injection times and weather conditions. This study presents one of the few systematic DO studies on artificial lagoons considering hydrodynamics and water quality issues. The results show a decrease in DO concentrations affected by high water temperatures. Further, the lagoons' hydrodynamic has a relevant impact on DO concentrations, e.g., tide wave induced DO concentrations to increase and decrease following a sinusoidal wave. Also, winds affect the DO propagation as low DO concentrations are obtained near the inflow boundaries. The outcomes demonstrate that DO concentrations depend on the lagoons' hydrodynamics, DO's production and consumption rate and tracer transport. The polluted water with low DO concentrations flowing from the desalination plant followed the wind direction. Besides, different quantities of binary and different injection times have minor effects on DO concentrations in the lagoons.

Keywords: TELEMAC-2D; water quality; dissolved oxygen; coastal lagoons; WAQTEL

1. Introduction

Coastal lagoons are considered unique and productive shallow water areas tightly linked to the sea or ocean through one or more inlet channels (Kennish and Paerl, 2010). Despite small areas of coastal lagoons, they have a noticeable impact on the genetic diversity of marine populations and the nearby sea conditions (Pérez-Ruzafa et al., 2019). Nowadays, coastal areas are under severe development pressure as they provide many natural services to societies; e.g., finfish and shellfish production, storm surge protection, tourism areas, anchorage, salt production and many other productive activities (Newton et al., 2018; Pérez-Ruzafa et al., 2019). Sewage from those human activities significantly alters water's physical, chemical, and biological characteristics to the degree that it cannot be used for the desired purposes (Pérez-Ruzafa et al., 2019). Moreover, the geographical location and the physical features of coastal lagoons make them highly impacted by their surrounding environment and more vulnerable to trophic imbalances (Chapman, 2012). Furthermore, the predicted climate change in the upcoming decades will add severe stress on their water quality.

Water quality and dissolved oxygen-related challenges are recently growing, affected by the increasing desalination byproduct discharged in marine systems (Ahmed and Anwar, 2012). Due to rapid industrialization, urbanization and other anthropogenic activities, water resources managers worldwide are pushing toward water desalination as a viable solution for water scarcity (Ahmed and Anwar, 2012). Recent estimates suggest that more than 100 million cubic meters of desalinated water are produced daily from approximately 16000 desalination plants in 177 countries worldwide (Jones et al., 2019). Those desalination plants alter the water characteristics of the nearby water system. For instance, water temperature adjacent to the brine disposal area increases and a high amount of nitrogen dioxide (NO_2), carbon monoxide (CO), Sulphur dioxide (SO_2) and nitric oxide (NO) is produced degrading the nearby water systems and their water quality (Ahmed & Anwar, 2012; Danoun, 2007). Besides, brine disposals have a high percentage of salinity, which, in turn, is inversely proportional to the Dissolved Oxygen (DO) concentrations (Haurwitz et al., 2008). The most commercially important desalination technology is reverse osmosis (RO) (Tularam and Ilahee, 2007). Compared to other desalination technologies, the brine from RO technology can cause fewer variations in DO concentrations due to relatively low-temperature variations (Lattemann and Höpner, 2008). On the other hand, mixing oxygen-consuming chemicals during the RO desalination process can reduce DO concentrations in water systems (Lattemann and Höpner, 2008).

Owing to the abovementioned threats to the water quality, preservation of the desired water quality and controlling the potential threats of freshwater in coastal areas has become an urgent challenge considering their complex physical processes, societal importance, desalination process and climate changes.

Due to water bodies' complexity and their nonlinear physical, chemical and biological characteristics, numerical water quality modelling techniques continuously gain importance. They can determine spatial and temporal variations of physical, chemical and biological states including critical conditions such as dissolved oxygen (DO) depletion or algae bloom. This can be conducted in less time and with lower costs when compared to in-situ investigations and traditional monitoring (Gholizadeh et al., 2016). Consequently, for the time being, several water quality models have been developed for simulating the present state, forecasting and assessing contaminant transport within, into and out of water bodies (Fu et al., 2019). For instance, SIMCAT, TOMCAT, QUAL2E, WAQTEL, QUASAR, MIKE-21 and ISIS are numerical modelling systems specialized in water quality investigations. The reliability and accuracy of such numerical models should be verified by comparing them with existing analytical solutions, which only exist for simple cases. Moreover, analytical and quasi-analytical approaches are still helpful for simplified analyses of contaminant transport when not sufficient data is available to warrant the use of a comprehensive numerical model, especially with the facility of new mathematical software such as Maple, Mathematica and Matlab (Van Genuchten et al., 2013).

Water quality models discuss different water properties such as DO, temperature, pH, conductivity, turbidity and total algae (Shamsudin et al., 2016). DO and its dropdown challenges are nowadays the focus of many systematic investigations. It is considered a crucial indicator of water quality, an essential element of aquatic systems and is involved in all metabolic processes (Abouelsaad et al., 2020; Gattuso et al., 2006). Studying the DO values helps prevent and control critical problems, namely oxygen-deficient and anoxic conditions, which occur if DO concentration is less than 6 mg/l and 2 mg/l, respectively and can destroy marine life (Mahaffey et al., 2020). Hypoxic conditions have become more common worldwide, especially in coastal areas and estuaries (Diaz and Rosenberg, 1995; Lee et al., 2021). In the last few decades, the dropdown of DO in coastal waters has dramatically increased due to the high observed temperatures and the high nutrient inputs affected by the growth of human activities (Breitburg et al., 2018). This problem of DO dropdown is expected to worse in the future due to rising water temperatures resulting from climate change.

In recent years, an increasing research interest lays on applying numerical techniques to investigate the DO and other water parameters in water bodies using different water quality models, e.g., (Bacon et al., 2017; Panda et al., 2015). Panda et al. (2015) used the MIKE-21 model to explore the hydrodynamics of the Chilika Lagoon located on the east coast of India coupled with a water quality model. They investigated water quality variables such as DO, salinity, temperature and nutrients. Their results agreed with the field-measured water quality variables so that their model can further predict future scenarios. In Kuwait, Bacon et al. (2017) applied the TELEMAC-2D water quality modelling system on the Sulaibikhat Bay. They concluded that their studied domain suffered from several fish-kill catastrophes in recent years due to a lack of oxygen (Bacon et al., 2017). Recently, researchers have tended to capture the complexities of the relation between the hydrodynamics of water bodies and the water quality parameters using field observations or numerical techniques (e.g., Huang et al., 2019; Marlina & Melyta, 2019; Pastore et al., 2019; Seiler et al., 2020). Huang et al. (2019) investigated the effect of three physical parameters of flow discharge, tide and wind data on the DO and the hypoxia events in the Pearl River estuary in China. They pointed out that the hypoxia area decreased with the reduction in river discharge during moderate or dry year scenarios. Also, a strong wind scenario can remarkably hinder the hypoxia propagation in the domain. Moreover, the DO concentrations had a wave of fluctuations over the spring-neap tidal cycles due to the vertical variation of water depths. Marlina and Melyta (2019) studied the influence of the speed of the wind, the cloud variation and the water temperature on Biochemical Oxygen Demand (BOD) and DO concentrations in the Winongo river in Korea. They found that the three studied parameters had a minor or no effect on BOD and DO, except the water temperature had a high effect on DO concentrations. Pastore et al. (2019) studied the relationship between the flow hydrodynamics from tidal waves and the water quality. Results show that higher values of DO were observed when larger tidal ranges were applied. Seiler et al., (2020) applied the MOHID 2D numerical model on the Patos lagoon in Brazil to assess the effect of wind and river discharge on water quality indicators. They found that the river discharge affected the northern and central lagoon areas, whereas the water quality in the estuaries area is influenced by wind force. In conclusion, the simulation of water quality of different coastal areas and the effect of the flow hydrodynamics on water characteristics nowadays attract much consideration in coastal areas, in which every domain shows its characteristics. On the contrary, the effect of desalination effluents on DO in coastal areas has not been comprehensively investigated yet, even though the research interest on desalinated water characteristics is rising.

El Gouna city is an attractive area for tourists and business activities, located on the Red Sea in Egypt. There are hotels, schools, golf clubs, ports, restaurants, which produce a lot of waste and wastewaters. Artificial coastal lagoons are widely constructed along the coast near El Gouna, seeking tourism attractions for economic purposes, often without examining their environmental impacts on the beautiful surrounding marine system (Rasul et al., 2019). Monitoring the water quality in El Gouna is an urgent action for the stability and preservation of that unique and precious environment. To the authors' knowledge, no numerical modelling investigating water quality in El Gouna has been yet developed. Previous studies (Abouelsaad et al., 2022) started from an assessment of bathymetry and tide field

measurements in El Gouna lagoons conducted by (Al-jabari, 2018) to then simulate and discuss the hydrodynamics of El Gouna lagoons and tracer transport under the effect of different weather conditions including variable tide, mean wind and maximum wind. In this work, a water quality model was applied in El Gouna lagoons considering their hydrodynamics using the TELEMAC-WAQTEL-O_2 model to investigate the DO concentrations and the impact of the organic load and the ammoniacal load on the DO concentrations. Physical processes of oxygenation, deoxidation and biochemical processes that alter oxygen production and consumption were discussed. This research aimed also to investigate the DO concentration considering the effect of different water temperatures and flow hydrodynamics under the impact of different weather conditions such as tide and wind. Further, this work analyzed the effect of binary polluted discharge from a nearby desalination plant on DO concentrations in the lagoons.

Firstly, the accuracy of the TELEMAC-WAQTEL-O_2 model was verified by comparing numerical results with analytical solutions for simple channels in both 1D and 2D flows using different constant and pulse injections of DO. After validating the TELEMAC-WAQTEL-O_2 model with numerical results, the TELEMAC-WAQTEL-O_2 model was applied to the more complex domain of El Gouna lagoons. A sensitivity analysis of the affecting parameters on DO was carried out to investigate their effect on the DO and ensure their plausibility. Furthermore, the spatial DO concentrations in the lagoons were computed in response to the variation of the water temperature, tide and wind. Finally, the negative effect of the nearby desalination plant on the DO concentration in the lagoons was investigated. Studying El Gouna artificial lagoons is crucial to preserve the water quality of the lagoons, which in turn protects the surrounding area of the Red Sea. This work sheds new light on the destructive impacts of desalination plants on coastal lagoons, and consequently on the marine ecosystem and its coral reefs.

2. TELEMAC-WAQTEL-O_2 Model

The hydrodynamic behavior of any coastal lagoon plays a significant role in its water quality characteristics. Consequently, for a related coupling with water quality model using TELEMAC-WAQTEL-O_2, complete hydrodynamics of the domain were firstly computed. The shallow water governing equations are the continuity equation, the momentum equations in x- and y- directions and the tracer transport equation (equations 1, 2, 3 and 4 in Appendix A1) (Hervouet and Ata, 2017). The wind blowing on the water surface is simulated in TELEMAC-2D, where the wind shear stress is considered through Flather's approach (Flather, 1976), as indicated in equations 7, 8 and 9 in the Appendix A1.

The model was then coupled with the O_2 water quality model. The O_2 model is a simple approach most recommended for short periods such as several days (Hervouet and Ata, 2017). In this model, co-inputs of organic load (L) and ammoniacal load (NH_4) wastes from treatment plants are considered without the full complexity of the manifold biological interactions and feedbacks (Bacon et al., 2017). It is restricted to modelling reaeration and the global oxidizable load. It does not consider the effect of planktonic plant photosynthesis and does not model the nitrogenous and phosphorus nutrients and their effect on phytoplankton. WAQTEL processor describes a source term that is added to the advection-diffusion equation resolved in TELEMAC-2D as follows (User manual of opensource software TELEMAC-2D V7P2, 2017):

$$\frac{\partial C_i}{\partial t} + u\frac{\partial C_i}{\partial x} + v\frac{\partial C_i}{\partial y} - \frac{\partial}{\partial x}\left(\nu_{t,t}\frac{\partial C_i}{\partial x}\right) - \frac{\partial}{\partial y}\left(\nu_{t,t}\frac{\partial C_i}{\partial y}\right) = F_i \quad (1)$$

Where C *is* tracer concentration (mg/l), u, v are velocity components in both flow directions (m/s), $\nu_{t,t}$ is turbulent diffusivity (m^2/s), F_i is a source or sink accounting for reactive transport and water quality interactions of respective tracer i (mg/l/d).

There are three tracers simply simulated in the O_2 model; DO, organic load (L) and ammoniacal load (NH_4), which vary according to the following laws:

$$F[O_2] = K_2(C_s - DO) - K_1\,[L] - K_4[NH_4] + P - R - \frac{BEN}{h} \quad (2)$$

$$F[L] = -K_1\,[L] \quad (3)$$
$$F[NH_4] = -K_4\,[NH_4] \quad (4)$$

Where K_2 is reaeration coefficient (d^{-1}), C_s is DO saturation concentration of water (mg/l), DO is dissolved oxygen concentration (mgDO/l), K_1 is a constant describing kinetic of degradation of organic load (d^{-1}), L is organic load (mg/l), K_4 is a constant of nitrification kinetic (d^{-1}), NH_4 is ammoniacal load (mg/l), P is photosynthesis (mgDO/d/l), R is vegetal respiration (mgDO/d/l), BEN is benthic demand (mgDO/m^2/day), h is water depth (m).

Generally, tracers can be classified as conservative or reactive tracers owing to their degree of interaction with the surrounding water or other tracers. A conservative tracer is affected only by dilution and diffusion without interaction with the water system. In contrast, reactive tracers interact and alter during their transport affected by different physical, chemical and biological processes (Cao et al., 2020). DO is considered a reactive tracer, whose levels result from the interaction among several processes, represented through different sources and sinks, which affect DO concentration, as indicated in equation 2 (Gualtieri and Gualtieri, 1999). DO enters the water through the air or is produced by the photosynthesis from phytoplankton, algae, seaweed and other aquatic plants (Watt, 2000). DO is consumed by the respiration of aquatic animals and the decomposition process driven by organic and ammoniacal load from wastewater. DO concentration in any water body depends on both the rate of oxygen production and consumption.

DO from the photosynthesis process is mainly produced on the water surface by algae and other shallow-water plants. Moreover, seaweed, sub-surface algae and phytoplankton can produce a high amount of oxygen underwater (Environmental, 2013). The photosynthesis process naturally depends on the light penetrating the water column, which depends on water depth (Venkiteswaran et al., 2007). Moreover, algal density is highly affecting oxygen production. Oxygen production from photosynthesis P often varies between 0.3 and 9 mgDO/d/l (User manual of opensource software TELEMAC-2D V7P2, 2017). Coastal zones can receive a significant amount of sunlight due to their shallowness (Gattuso et al., 2006). In this regard, the photosynthesis process plays a significant role in DO production in coastal areas.

Reaeration is the physical absorption of oxygen from the atmosphere by water. It is considered the main source of oxygen production, especially in rivers and streams, by which DO conditions in any water domain can improve. The rate of mass transfer of oxygen is equal to $K_2(C_s - DO)$, as shown in the first terms of equation 2 (Thomann and Mueller, 1987).

Haider et al. (2013) divided reaeration equations for calculations of the K_2 coefficient into four groups depending on the number of the parameters affecting the reaeration coefficient value (Haider et al., 2013). In this subdivision, reaeration is influenced by water depth, velocity, the slope of the stream, diffusion coefficient, kinematic viscosity, Froude or Reynolds number and head loss. In the TELEMAC-WAQTEL-O_2 model, four formulas can be chosen for calculating the reaeration coefficient: the formula of Tenessee Valley Authority (Authority, 1972), the formula of Owens et al. (Owens and Innis, 1999), the formula of Churchill et al. (Churchill et al., 1964) or the formula of O'Connor & Dobbins (O'Connor and Dobbins, 1958). A final formula that combines the three last formulas is also available in the TELEMAC-WAQTEL-O_2 model, where choosing the K_2 formula depends on the water depth and velocity at each point of the mesh (User manual of opensource software TELEMAC-2D V7P2, 2017). For all discussed K_2 formulas, the value of K_2 is inversely proportional to water depth and directly proportional to flow velocity, as indicated in equations 15 to 20 in Appendix A3. Also, the calculated reaeration coefficient is determined at 20°C. Correction of the temperature variation is computed as:

$$(K_2)_T = (K_2)_{20°C}(\theta^{T-20}) \quad (5)$$

Holley (1975) suggested that the value of θ ranges between 1.005 and 1.030 (Holley and Liggett, 1975) while the most common θ value is 1.024 (Haider et al., 2013). This value is also recommended and chosen in TELEMAC.

Further, the oxygen saturation concentration of water (C_s) is mainly dependent on the temperature. TELEMAC-WAQTEL offers the two most common formulas to calculate C_s: the formula of Elmore & Hayes or the formula of

Montgomery (Richardson et al., 2001), as shown in equations 22 and 23 in Appendix A3. Finally, the benthic demand (BEN) ranges from 0.007 to 7.0 gDO/m^2/day depending mainly on the bed soil's type ("WAQTEL," 2020). Benthic demand also depends on water temperature and is correlated considering different water temperatures.

3. Model Verification with Analytical Solutions

The transport of tracers in the water is described with an advection-diffusion equation including external and internal sources and sinks. Analytical solutions for calculations of DO and its transport can consider advection, diffusion and the different DO production and consumption parameters. The analytical solutions of some simple hydrodynamic cases (stagnant water, 1D flow) under the effect of a pulse or constant injection of DO were compared with the corresponding TELEMAC-WAQTEL-O_2 results to verify the outcomes. Some mandatory simplifications were applied such as using constant values for the flow velocity and the longitudinal dispersion and adopting idealized initial and boundary conditions.

The equation controlling the DO concentration in stagnant water is indicated in equation 6 (simplification of equation 1). While equation 7 describes the analytical solution considering only the effect of reaeration coefficient (K_2) and saturation concentration of water (C_s) neglecting other production and consumption parameters as follows:

$$\frac{\partial O_2}{\partial t} = K_2(C_s - [DO]) - K_1\,[L] - K_4[NH_4] + P - R - \frac{BEN}{h} \quad (6)$$

$$DO(t) = \ (DO_0 - C_S) * e^{-K_2 * t} + C_S \quad (7)$$

Where $DO(t)$ is the unknown DO concentration at time t (mgDO/l) DO_o is the initial DO (mgDO/l).

Firstly, two cases for a simple domain of stagnant water with zero flow velocity were compared with analytical results for 4 days of simulation with an initial DO concentration of 5 mg/l to individually capture the impact of degradation of DO affected by different production and consumption parameters. For the first case, the effect of the reaeration coefficient was individually discussed neglecting all other parameters. For the second more complex case, the addition effect of saturation density of oxygen (C_s) to the reaeration load was investigated (equation 7) and compared with the corresponding analytical results. The applied values of C_s and K_2 were 11 mgDO/l, and 0.9 day $^{-1}$, respectively.

Afterwards, a 400-m long one-dimensional domain with a water depth of 1 m and a constant small flow velocity of 0.001 m/s was discussed. The initial DO concentration was assumed to be zero, while a pulse and a continuous DO concentration equal to 5 mgDO/l was injected. The resultant DO concentrations were compared in both cases with the analytical results after Kinzelbach (1992) (equations 10, 11 and 12 in Appendix A2).

The DO concentrations were calculated for 4 days considering a simplified degradation coefficient considering only reaeration (i.e., degradation coefficient $= k_2$). For the pulse injection, DO was injected only for 1 s at the beginning of the simulation, while DO was injected continuously for 4 days in case of constant injection. Also, the retardation coefficient (equation 10, 11 and 12 in Appendix A2) was assumed to equal 1.

Finally, a 2D channel with a water depth of 10 m and a constant horizontal flow velocity was discussed. The initial DO concentration was assumed to be zero. The 2D tracer transport equation for DO was analytically determined according to Kinzelbach (1992), as shown in equations 13 and 14 in Appendix A2. The retardation coefficient was assumed to equal 1, while the degradation was simplified and affected by reaeration only (i.e., degradation coefficient $= k_2$). A constant DO injection with 5 mgDO/l with a flow velocity of 0.001 m/s was injected for a study period of 4 days.

A further aspect can also help verify our simulation results using TELEMAC-WAQTEL-O_2 by comparing the simulated DO concentrations with saturation DO values at different water temperatures. Due to high atmospheric contact, shallow water such as El Gouna lagoons remains close to 100 % saturation (Wetzel, 2001). Also, DO in shallow water can often achieve levels over 100 % saturation due to photosynthesis and aeration (Wetzel, 2001). In this regard,

the average simulated DO concentrations in the lagoons were compared with the corresponding DO saturation values at different water temperatures ranging from 16 to 30°C.

4. Study Area and Data

The charming touristic city El Gouna, located in Egypt, is a network of interconnected artificial lagoons linked to the western branch of the Red Sea. Those lagoons are characterized by a wealth of natural heritage and resources such as coral reefs and marine life (Gurguess et al., 2009). El Gouna artificial lagoons created a new environment for tourism activities, which enriched El Gouna city. Those artificial lagoons are negatively affected by hotels' sewage outflow, touristic and local wastes and boat leakages (Al-Jabari, 2018). Moreover, in El Gouna city as a self-sufficient city, three desalination plants were recently constructed to provide a new source of desalinated water used in various tourism and economical activities (Jahnke et al., 2019). The three desalination plants produce daily from 4000 to 6000 m^3 of desalinized water with brine wastes of 6000 to 8000 m^3 (Jahnke et al., 2019). The three desalination plants mentioned above use RO technology for the desalination process. Direct discharge of brine from the desalination plants into the neighboring Red Sea is forbidden by law. Consequently, El Gouna's studied artificial lagoons receive a harmful part of the brine discharged from the desalination system in the city (Jahnke et al., 2019).

Geometrically, the studied domain consists of two connected lagoons with a perimeter of approximately 4700 m and a surface area of 230,000 m^2 with a mean water depth of less than 3 m. The restricted lagoons of El Gouna exchange their water with the Red Sea through three narrow inlets for water inflow and outflow. The brine disposal from the nearby desalination plant enters the lagoons through the temporary water inlet in the middle of the left side and is considered the primary source of contamination in the studied lagoons. Fig. 1 shows the studied domain of the El Gouna lagoons in Egypt, water depths and the four above-mentioned water inlets.

This study depended on field data for El Gouna lagoons considering the bathymetry and the tide from a previous assessment study (Al-Jabari, 2018). The author tracked and investigated water depths of approximately 1700 points inside the lagoons and estimated the fluctuations of water level due to the tide force as a sinusoidal wave, wherein every tide wave had a peak-to-peak amplitude of 0.6 m repeated two times daily. The weighted average wind speed and wind direction were calculated by (Abouelsaad et al., 2022), in which data about monthly wind data were collected from the weather station beside the domain for a period of two years from 2015 to 2017. The mean applied wind speed and direction were calculated to be equal to 5.84 m/from the northwest direction. Also, the lagoons are subjected to a maximum wind speed of 20.8 m/s from the southeast (Abouelsaad et al., 2022).

5. Model Parameters and Simulation Scenarios

5.1. Model setup

During a complete modelling process using TELEMAC-2D, pre-and post-processing tools are used for mesh generation, assigning boundary conditions and visualization of results. Janet software developed by Smile Consult GmbH (Lippert, 2001) was used for mesh generation and creation of boundary conditions files. The created Janet mesh was composed of 4800 triangular elements, 2700 nodes and 7500 edges approximately. This mesh was chosen after achieving a good grid convergence in low computation time. Moreover, the constructed mesh obtained similar results with a refined mesh. On the other hand, the ParaView post-processing tool was used to visualize output results from TELEMAC-2D.

For simulations using TELEMAC-2D, a constant value of 12.0 m water elevation and zero flow velocities were used as initial conditions for the whole domain. For the boundary conditions, three exchange locations with the Red Sea were simulated as Dirichlet boundary conditions for water levels affected by tide waves. Also, a Dirichlet boundary

condition of brine discharge and tracer concentration from the desalination plant in the middle of the left side of the domain was adopted.

For the simulation of the hydrodynamic properties of the domain using TELEMAC 2D, the following numerical approaches were used. The method of characteristics was used to solve the Saint-Venant equations applying linear discretization for the water velocity and tracer, while water depths were calculated using the PSI method. For bottom friction, Strickler's law with a magnitude of 40 $m^{1/3}/s$ was adopted (equations 5 and 6 in Appendix A1). The constant viscosity turbulence model was applied with a turbulent viscosity coefficient of 10^{-4} m^2/s. The turbulent diffusivity was set equal to the turbulent viscosity. The impact of the turbulence was predicted to be small, especially in such shallow water, therefore remarkable changes were not expected with applying more advanced models, which would need more CPU time such as k-epsilon model or Elder model. The prescribed values for bottom friction, viscosity and numerical schemes were obtained from a previous study carried out by (Abouelsaad et al., 2022).

TELEMAC-2D was then combined with the WAQTEL-O_2 model to calculate the concentration of DO in El Gouna lagoons. A separate steering file was created to describe the different physical and biochemical processes of consuming and producing DO. Field data about water quality in the studied lagoons are not available. Consequently, the background value of DO is considered from a previous field study for the Red Sea in 2016 (nearby section from the lagoons located in 27°11'37.5" 33°56'12.6") (Fahmy et al., 2016). Average values of approximately 8 mgDO/l, 2 mgDO/l and 0.01 mgDO/l for DO, organic load and ammoniacal load, respectively, at 26°C for water temperature were adopted. The default values of the degradation constant of the organic load (K_1) and the constant of nitrification (K_4) were applied equal to 0.25 d^{-1} and 0.35 d^{-1} (equation 2). Vegetal respiration (R) also was kept at its default value of 0.06 mgDO/l. The default benthic demand (BEN) of 0.1 mgDO/l was corrected depending on the applied water temperature (Hervouet and Ata, 2017).

5.2 Simulation scenarios

Due to the lack of field measurements to assess the spatial DO in the studied lagoons, a sensitivity analysis of the effect of different input parameters on the DO concentration was conducted under the effect of tide and mean wind over a simulation period of 8 days. E.g., photosynthesis value within its reference ranges (described in sec.3), the presence of the organic load and the ammoniacal load effect and the two formulas for computing C_s were compared. Although no data for model calibration were available, we gained an insight into how the water quality was influenced by changes in chosen values, formulas and conditions in reasonable ranges considering initial DO concentrations, organic load and ammoniacal load from the previous field investigation in the Red Sea near the lagoons.

Further, a numerical simulation of the DO in the lagoons under different water temperatures and different weather conditions of tide and wind was conducted. Moreover, the propagation of the brine discharge and its effect on the water quality of the lagoons were simulated under the effect of different weather conditions. Before the latter mentioned simulations, a sensitivity analysis of different binary discharges, different DO concentrations in binary discharge and different injection times of brines was investigated. The details are illustrated in Table 1 for the sake of synthesis along with the abbreviations used to indicate the scenarios. Every scenario will be presented in detail in the following section. In particular, the simulated cases are divided into hydrodynamic and brine transport ones: the former scenarios focus on the DO variations under different weather conditions, the latter ones consider the transport of effluent discharge from the nearby desalination plant for 8 days. This study gives an overview of the DO values in the lagoons and recommendations for brine injection.

The DO concentration was analyzed for all simulation scenarios in 7 observation points shown in Fig. 1, in which the numbers of points represent their IDs. They were chosen to represent results in relevant locations for the study scopes. For instance, points 1914, 1073 are next to the two bottom boundaries with the Red Sea, point 2600 is

near the upper right flow boundary and point 1051 is on the upper side of the desalination plant's inflow. Contrary points 2260 and 193 are inner points and point 1391 is in the narrowest section of the domain.

Table 1: Hydrodynamics and brine transport scenarios for a simulation duration of 8 days

	Name of scenario	Description
Hydrodynamics (Temperature, tide and wind)	DO-T20	DO concentrations under the effect of air temperature equals 20 $^{\circ}$C
	DO-T25	DO concentrations under the effect of air temperature equals 25 $^{\circ}$C
	DO-T30	DO concentrations under the effect of air temperature equals 30 $^{\circ}$C
	DO-TIDE-MW	DO concentrations under the effect of tide and mean wind
	DO-TIDE	DO concentrations under the effect of tide
	DO-MW	DO concentrations under the effect of mean wind
	DO-MAXW	DO concentrations under the effect of maximum wind
Brine transport	BRI-ZERO	DO concentrations considering no effluent discharge from desalination plant
	BRI-DO7	DO simulations under brine discharge from desalination plant of 0.2 m^3/s with DO of 7 mgDO/l
	BRI-DO5	DO simulations under brine discharge from desalination plant of 0.2 m^3/s with DO of 5 mgDO/l
	BRI-DO3	DO simulations under brine discharge from desalination plant of 0.2 m^3/s with DO of 3 mgDO/l
	BRI-HQ3	DO simulations under high brine discharge from desalination plant of 0.2 m^3/s for 3 hours daily
	BRI-MQ6	DO simulations under intermediate brine discharge from desalination plant of 0.1 m^3/s for 6 hours daily
	BRI-LQ12	DO simulations under low brine discharge from desalination plant of 0.05 m^3/s for 12 hours daily
	BRI-HSTQ3	DO simulations under binary discharge from desalination plant of highest discharge of 0.4 m^3/s for 3 hours daily
	BRI-TIDE	Brine DO simulations under the effect of tide
	BRI-MW	Brine DO simulations under the effect of the mean wind
	BRI-MAXW	Brine DO simulations under the effect of the maximum wind

6. Results and Discussion

6.1 Model Verification with Analytical Solutions

The TELEMAC-WAQTEL-O2 model was firstly verified by comparing the model results with simple analytical solutions of some hydrodynamic cases (stagnant water, 1D flow) under the effect of a pulse or constant injection of DO. Firstly, two cases for a simple domain of stagnant water were compared with analytical results. The individual effect of the reaeration coefficient and the effect of saturation density of oxygen (C_s) and the reaeration load compared to the analytical results are shown in Fig. 2. It can be concluded from the figure that the numerically calculated DO coincides with the analytical solution for stagnant water in both cases.

Afterwards, the DO concentrations using the TELEMAC-WAQTEL-O2 model were compared with analytical solution for different 1D and 2D domains using a pulse and a constant injection of tracer for 4 days of simulation. Reasonable and quasi-steady state results are obtained within this period, therefore, there was no need to make the simulations longer than 4 days.

n 1D model are shown in Fig. 3. It can be noticed from Fig.3-a that there are some deviations affected by a little damping that occurred in the early stage of simulation of point injection having a relatively high error of about 15% in the beginning of the domain. While, the average error percentages in case of pulse and constant injection over

the whole simulation period range from less than 1% to not more than 4%. It can be concluded that both investigated cases show that the numerically calculated deviation of the DO reasonably coincides with the analytical solution with a small time-shift between both results. Moreover, for the 2D domain, the comparison between the DO concentrations in different selected points in the middle of the domain width at different distances along the x-axis for both the analytical and numerical results is shown in Fig. 4. It can be concluded from the figure that the DO concentrations calculated from analytical solutions and simulation results show a good agreement with a small acceptable time-shift between both results. The average error percentages decrease with distance to reach percentages of less than 4% after less than 50 m from the inflow of the domain. As a conclusion, the similar trend of the DO concentration in a simple water domain for both the TELEMAC-WAQTEL-O_2 model and the analytical solution for different 1D and 2D cases supports applying the prescribed model to more complicated domains, for which no analytical solutions exist.

On the other hand, the TELEMAC-WAQTEL-O2 model was also verified by comparing the average simulated DO concentrations in the lagoons with the corresponding DO saturation values at different water temperatures ranging from 16 to 30°C, as shown in Fig. 5. It can be seen from Fig. 5 that the DO concentrations in the lagoons reach the saturation level of DO and achieve levels over 100 % saturation at high water temperatures affected by photosynthesis and reaeration.

6.2 Sensitivity analysis of water quality parameters

6.2.1 Photosynthesis

In coastal areas, the photosynthesis process has a significant impact on DO production. There has been no detailed investigation of the algae's existence and other plants producing oxygen in the studied lagoons. Consequently, the DO concentration in the lagoons was investigated assuming different photosynthesis values of 0.3, 1, 9 mgDO/l as suggested by TELEMAC-2D (Hervouet and Ata, 2017) under the effect of tide with mean wind. The DO concentration was also investigated ignoring the effect of photosynthesis, i.e., P = 0. The temperature was assumed to be constant at 20°C. Also, the effect of both the organic load and the ammoniacal load was neglected. Table 2 illustrates the DO values in the lagoons for the photosynthesis values mentioned above. Also, the variation percentages of average DO concentrations compared to the reference values used in TELEMAC model (P = 1.0 mgDO/l) are indicated in Table 2.

Table 2: Average DO concentrations (mgDO/l) and percentage of variation for different photosynthesis values (0.0, 0.3, 1.0, 9.0 mgDO/l) at the observation points and the whole domain

Average DO (mgDO/l)	Point 2600	Point 2260	Point 193	Point 1051	Point 1391	Point 1914	Point 1073	Average (% variation)
P = 0.0 mgDO/l	8.50	8.70	8.54	8.56	8.61	8.66	8.65	8.60 (10.3%)
P = 0.3mgDO/l	8.65	8.92	8.85	8.75	8.80	8.89	8.88	9.03 (5.8%)
P = 1.0 mgDO/l	9.11	9.77	9.83	9.35	9.43	9.82	9.77	9.59
P = 9.0 mgDO/l	17.3	21.22	24.16	18.98	20.21	24.41	23.7	27.1 (182.6%)

It can be observed from Table 2 that photosynthesis plays an obvious role in DO production in the lagoons. For instance, the minimum activity of the photosynthesis process (P = 0.3 mgDO/l) increases the average DO from 8.60 mgDO/l in case of no photosynthesis activity to 9.03 mgDO/l in 8 days. While with high photosynthesis' DO production (P = 9.0 mgDO/l), the average DO is more than its triple initial value and reached a value of 27.1 mgDO/l (with % increase of 182.58%). However, very high DO concentrations are harmful to fish, as they can cause gas bubble disease (Environmental, 2013). The optimum DO rate is around 5-8 mg/l and increases to 4-15 mg/l beside coral reefs owing to the day photosynthesis production and night plant respiration (Talley, 2000). For the scenarios presented in the next sections, the photosynthesis indicator value was chosen to equal 1 mgDO/l as an average value (“WAQTEL,” 2020).

6.2.2 Cs formulas

Oxygen saturation density of water (C_s) can be accounted for in the TELEMAC-WAQTEL-O_2 model using two different formulas, one of Elmore and Hayes and another of Montgomery. It is found that both formulas for calculating the oxygen saturation density of water gave very similar values at all observation points. The average C_s values considering both formulas are 9.26 and 9.30 mg/l under the effect of tide with mean wind. Consequently, simulating the DO using any of the two methods is adequate. For the next investigated scenarios, the formula of Elmore and Hayes was chosen to calculate the oxygen saturation density of water (C_s).

6.2.3 Organic load and ammoniacal load

Both organic load and ammoniacal load negatively disturb the DO concentrations through the decomposition process. In this regard, DO concentrations in the lagoons were investigated through three scenarios: no ammoniacal load, no organic load and presence of both loads of organic load and ammoniacal load with initial values of 2.0 mgDO/l and 0.01 mgDO/l, respectively. Initial DO concentration of 8 mgDO/l was adopted for the entire domain.

It is found that the presence of the ammoniacal load did not change the DO concentration at any of the observation points due to its small initial amount. On the other hand, the organic load had a relatively higher impact as it diminished the total average DO from 9.59 to 9.26 mg/l with a decrease percentage of 3.5 % under the effect of tide with mean wind.

For the scenarios presented in the next sections, the effect of organic load and the ammoniacal load was neglected to isolate the effect of different weather conditions and water temperatures on the reaeration, which, in turn, affects the DO concentrations.

6.3 Temperature impacts

The average water temperature in El Gouna city is calculated to be approximately 25°C with a minimum average value of approximately 20°C in February and a maximum average value of 30°C in July. These temperatures were calculated based on the data over the years 2009 to 2019 from online available weather data for El Gouna city. The DO concentrations in the lagoons were examined under three temperatures: 20°C, 25°C and 30°C (DO-T20, DO-T25, DO-T30 scenarios). In TELEMAC, both reaeration and benthic demand are directly influenced by any change in water temperature. Table 3 illustrates the DO values at the observation points for the aforementioned water temperatures. Also, the variation percentages of average DO concentrations compared to the average temperature (T = 25°C) are indicated in Table 3. While Fig. 6 compares the quantities of DO in the whole domain at 20°C and 30°C at the end of the simulation period of 8 days.

Table 3: DO concentrations (mgDO/l) for different water temperatures (20°C, 25°C, 30°C) at the observation points and the average value (showing the % variation) in the whole domain

Average DO (mgDO/l)	Point 2600	Point 2260	Point 193	Point 1051	Point 1391	Point 1914	Point 1073	Average (% variation)
DO-T20	8.91	9.45	9.42	9.09	9.14	9.42	9.38	9.26
DO-T25	8.03	8.64	8.61	8.24	8.29	8.58	8.54	8.41 (10.1%)
DO-T30	7.25	7.94	7.93	7.50	7.55	7.88	7.84	7.69 (17.0%)

It can be observed from Table 3 that the DO concentration is inversely proportional to the water temperature. For instance, the average DO concentration is 9.26 mg/l at 20°C while 7.69 mg/l at 30°C. In other words, while increasing water temperature by 5°C and 10°C above 20°C, the total average DO values decrease by 10% and 17%,

respectively. Besides, as indicated in Fig. 6, the DO concentrations decrease in the lagoons to reach a value lower than 6 mgDO/l at an area in the north-eastern side due to the increase in the water temperature, while in the case of low temperatures, the minimum DO value is 8 mgDO/l. The reason behind the increase or the decrease of DO is the effect of water temperature on reaeration coefficient (K_2), oxygen saturation density of water (C_s) and benthic demand (BEN) as indicated in equations mentioned in the Appendix A3.

6.4 Hydrodynamic impacts

The difference in DO concentrations between different locations in the computational domain under the same conditions is influenced by the changes in the flow hydrodynamics of velocity and water depth at each observation point. In this regard, a focus on the impact of the bathymetry and the hydrodynamics of the lagoons on DO concentrations was investigated. Table 4 illustrates the average DO concentrations and the corresponding water depths and velocities at each observation point under the effect of the tide with mean wind (DO-TIDE-MW scenario).

Table 4: DO concentrations (mgDO/l), water depths (m) and velocities (m/s) at the observation point under the effect of tide and mean wind

	Point 2600	Point 193	Point 1051	Point 1391	Point 1914	Point 1073	Average
DO (mgDO/l)	8.35	8.16	8.34	8.47	8.41	8.04	8.36
h (m)	1.59	2.10	1.57	1.32	1,02	1.36	1.26
V (m/s)	0.06	0.01	0.02	0.02	0.02	0.03	0.02

Further, Fig. 7 illustrates the course of the DO concentrations at the observation points over the 8 days of simulation. The mentioned spatial and temporal DO concentrations correspond to the water depth and flow velocities computed by (Abouelsaad et al., 2022). It can be observed from Table 4 and Fig. 7 that the DO distribution in the lagoons not only depends on DO production and consumption processes affected directly by water depths and velocities, but the location of the observation points also has a significant influence on DO concentrations as a tracer. The final DO distribution in the lagoons follows complex dynamics depending on locations, hydrodynamics and tracer governing law. For instance, while comparing point 2600 and point 1051, which have approximately the same water depth and the same DO concentration, despite that point 2600 has a velocity value of three times the velocity at point 1051. This is caused due to the distance of point 1051 from the open boundaries compared to the location of point 2600. In this regard, the DO in the lagoons was investigated under different weather condition scenarios (DO-TIDE, DO-MW and DO-MAXW) to explore further the DO dynamics.

6.4.1 Tide impacts

DO concentrations in the lagoons were calculated under the effect of the tide wave only, in which every tide wave has an amplitude of 0.6 m and is repeated twice every day. The mean water depth of about 3m corresponds to a water level elevation of about 12m above mean seal level (as shown in Fig. 8). Table 5 investigates the average DO concentrations, water depths and velocities under the impact of the tidal wave. Moreover, Fig. 8 shows the fluctuation of DO concentrations for all observation points compared to the applied tide wave

Table 5: Comparison between DO concentrations (mgDO/l) and corresponding water depths (m) and velocities (m/s) at the observation points under the effect of DO-TIDE scenario

		2600	193	1051	1391	1914	1073	Average
DO-TIDE	DO (mgDO/l)	10.59	10.90	11.06	11.02	11.23	10.80	10.83
	h (m)	1.59	2.10	1.57	1.32	1.02	1.36	1.26
	V (m/s)	0.03	0.01	0.01	0.01	0.02	0.04	0.01

From Table 5, it can be noticed that the DO concentrations in the whole domain have average values ranging from 10.6 mgDO/l to 11.2 mgDO/l approximately, although they have different attitude against the effect of rises and falls of the tide wave. Point 2600 and point 1073 show relatively low DO concentrations of 10.59 and 10.80 owing to their location near boundary conditions despite their relatively high velocities. On the other hand, point 1914 near the third boundary has a high DO concentration due to very low water depth, which is inversely proportional to the reaeration value. It can be noticed from Fig. 8 that the tide wave greatly influences the DO in the lagoons. It rises and falls inversely to the tidal wave. For instance, the low values of DO occur at high water depths due to the inverse relationship between them and the reaeration.

6.4.2 Wind scenarios

Mean wind condition

From the hydrodynamics of the lagoons under the effect of mean wind, the water depths were slightly affected by the wind. The water flux tended to run regularly into the domain from the top right open boundary and go out from both bottom boundaries with a small mean velocity of less than 0.03 m/s (Abouelsaad et al., 2022). DO concentrations showing the hydrodynamic behavior of the domain after 8 days are illustrated in Fig. 9. Moreover, Fig 10 presents the DO concentrations at each observation point for the whole study period.

Due to the wind's small effect on the hydrodynamics of the lagoons, small amounts of DO production, consumption, and tracer outflow were observed. Consequently, the DO concentrations at all observation points, except for point 2260, have a low increasing rate as shown in Fig. 10. Also, an average DO concentration of 9.30 mgDO/l was observed in DO-MW scenario with no waves of increase and decrease in any observation point as occurred in the DO-TIDE scenario. The direction of flow is significantly influencing the DO concentrations. For instance, points near the top inflow boundary have the lowest DO values such as point 2600. Also, points away from the inflow direction have high DO concentrations such as points 1073 and 1914, as shown in Fig. 9. Point 2260 shows a higher retention time of DO tracer and an increasing rate. This point is in fact located in the remotest area from the three boundaries; thus, the produced oxygen was longer retained in the area.

Maximum wind condition

The hydrodynamic results of the maximum wind scenario showed a negligible effect on the water depths, while the flow velocities reached a relatively high mean value of 0.2 m/s (Abouelsaad et al., 2022). Also, the water flux regularly ran into the domain from the two bottom boundaries and flowed out from the top right boundary. DO concentrations under the aforementioned hydrodynamics after 8 days of simulations are illustrated in Fig. 11. Also, Fig. 12 presents the DO concentrations at each observation point for the whole study period.

Owing to the high flow velocities, the DO retention time decreased yielding to a mean DO concentration of 8.47 mgDO/l, despite the high DO production rate affected by high flow velocities. Fig. 12 illustrates that there are no fluctuations of wave-like rise and fall in DO in all observation points, as observed in the DO-TIDE scenario. Also, the flow direction affects the DO concentrations, in which points near the inflow bottom boundaries have lower DO concentrations when compared to higher values in the top of the domain near the outflow top right boundary, as shown in Fig. 11.

Finally, the effect of DO-TIDE, DO-MW, DO-MAXW scenarios on the average DO concentration was compared as illustrated in Table 6.

Table 6: Comparison of DO concentrations mgDO/l) and corresponding water depths (m) and velocities (m/s) under the effect of different weather conditions (DO-TIDE, DO-MW and DO-MAXW).

Average	DO-TIDE	DO-MW	DO-MAXW
DO (mgDO/l)	10.83	9.30	8.47
h (m)	1.26	1.26	1.26
V (m/s)	0.01	0.02	0.11

As can be observed in Table 6, the DO-MAXW scenario results in the lowest mean DO concentrations, despite high velocities and high reaeration rates. On the contrary, although tide wave has lower flow velocities and consequently low reaeration, the average value of DO highly increases. These results demonstrate that the total amount of DO not only depends on the reaeration and DO consumption and production rate but also on the water residence time, which had a relevant effect on DO concentrations.

6.5 Brine discharge impacts

6.5.1 Sensitivity analysis on DO concentration in brine discharge

The brine discharge enters the domain from the nearby desalination plant through the open middle left boundary near the desalination plant, as shown in Fig. 1. DO concentrations values in the effluent are not available. For this reason, four scenarios (BRI-ZERO, BRI-DO7, BRI-DO5 and BRI-DO3) were compared changing the DO values in the brine discharge, assumed equal to 0.2 m^3/s. The average DO values after 8 days of simulation in the lagoons were equal 9.67, 9.42, 9.32, 9.23 mgDO/l, respectively for the above-mentioned scenarios affected by low brine DO concentrations. Fig. 13 presents the comparison among four observation points of two scenarios: BRI-ZERO, BRI-DO3, where only the bottom left side of the lagoons was highly affected by the brine discharge. E.g., point 845, which is just next to the effluent inflow from the desalination plant (as shown in Fig. 1), shows a decrease of DO concentration from 10 mgDO/l approximately to less than 8 mgDO/l. Also, DO concentration at point 1073 decreased by approximately 0.4 mgDO/l in 8 days. While point 1914 and point 2600 show minor differences in the two scenarios.

6.5.2 Sensitivity analysis on brine injection times and different brine discharges

The same total quantity of binary discharges with the same DO initial concentration were considered with different injection times considering BRI-HQ3, BRI-MQ6 and BRI-LQ12 scenarios. Also, the effect of changing the quantity of binary discharge was investigated by comparing BRI-HQ3 and BRI-HSTQ3 scenarios. The average DO concentrations were equal to 9.62, 9.64, 9.72 and 9.62 mgDO/l for the mentioned scenarios, respectively. Increasing the injection time or increasing the binary quantity had minor effects on DO concentrations.

6.5.3 Different weather conditions

A comparison between the dispersion of the brackish water from the desalination plant effluent under different weather conditions, considering BRI-TIDE, BRI-MW and BRI-MAXW scenarios for 5 days of simulation is presented in Fig. 14. The applied weather condition significantly influenced the DO tracer movement. It mainly concentrated beside the desalination plant boundary and went slightly upward to leave from the top right boundary in the BRI-TIDE scenario. It followed mainly the same direction of the mean wind to leave the domain from the left bottom boundary in the second scenario. Finally, the maximum wind direction drove the tracer upwardly, similar to the tide case with a rapid outflow rate.

7. Conclusions

A 2D vertically averaged water quality numerical model has been set up using the TELEMAC-WAQTEL-O_2 model to investigate the water quality of artificial lagoons in El Gouna city, Egypt, with the focus on the distribution of DO concentrations. This research aimed to explore the DO concentration considering the effect of water temperature and flow hydrodynamics (tide and wind). Also, the effect of the binary polluted discharge from a nearby desalination plant on DO concentrations was analyzed.

Firstly, analytical solutions for the DO in simple 1D and 2D domains have been discussed and compared with the corresponding numerical results considering the impacts of stagnant water, a pulse and a constant injection of DO. Good agreements between numerical and analytical solutions were obtained, which ensured the ability of the TELEMAC-WAQTEL-O_2 model in simulating the complex domain of El Gouna lagoons.

Secondly, a sensitivity analysis was conducted to assess the impact of varying model input factors, such as photosynthesis, formulas for calculating oxygen saturation concentration of water C_s, organic load and ammoniacal load. The sensitivity analysis demonstrates a considerable positive effect of the photosynthesis process on DO increase. Moreover, organic load produces a relatively high negative effect on the average DO compared to the ammoniacal load's negligible effect. Also, applying both formulas for computing C_s gives similar results.

Afterwards, the domain was investigated considering different temperatures, which resulted in being inversely proportional to DO. Specifically, the DO average concentration decreased from 9.26 to 7.69 mgDO/l when the water temperature increased from 20°C to 30°C. Also, different tide and wind scenarios were simulated: (1) tide, (2) mean and (3) maximum wind. The tide wave creates a sinusoidal wave of DO concentrations which behaved inversely proportional to the changes in the water depths. Moreover, the direction of the mean and maximum wind speed greatly affects the DO values in all observation points. E.g., the points beside the water inflow present low DO values compared with the high DO values beside outflow points. Finally, comparing the weather conditions scenarios, it is found that DO retention is controlled by water residence time and the hydrodynamics of the system, which in turn affects the reaeration rate. Although the DO reaerations are relatively low in tide and mean wind scenarios compared to the maximum wind one, they have a higher DO residence time.

Exploring the impact of the binary tracer discharge emissions from the nearby desalination plant, it is found that the average DO in the lagoons decreases, especially in the bottom left area, from 9.67 to 9.23 mgDO/l due to a low concentration of DO in desalinated water equal to 3 mg/l. Besides, different quantities of tracer and different injection times have minor effects on the DO concentrations in the lagoons. Finally, the propagation of binary effluent with low DO concentrations is discussed considering three scenarios (tide only, mean wind only and the maximum wind only), in which the polluted water with low DO concentrations is always found to follow the flow direction. In case of only tide forcing, the polluted water is concentrated next to the desalination plant.

This work is considered a preliminary and fundamental step for a complete insight of water quality in El Gouna artificial lagoons and their environmental preservation. Having a broader picture of the water quality in the lagoons is an essential component to initiate discussions with stakeholders and decision-makers in the area and embrace mitigation actions to protect the El Gouna gorgeous environment and its surrounding coral reefs.

Acknowledgment

The authors would like to express their gratitude to the Cultural Affairs and Missions Sector, Ministry of Higher Education in Egypt for their regular support.

References

Abouelsaad, O., Abdallah, K., Matta, E., Porst, G., Omar, M., Hinkelmann, R., 2020. Numerical simulation of dissolved oxygen in coastal lagoons Case study: El Gouna, Egypt.

Abouelsaad, O., Matta, E., Hinkelmann, R., 2022. Hhydrodynamic response of artificial lagoons considering tide, wind and tracer–case study El Gouna, Egypt. Regional Studies in Marine Science 102290.

Ahmed, M., Anwar, R., 2012. An Assesment of the Environmental Impact of Brine Disposal in Marine Environment. International Journal of Modern Engineering Research 2, 2756–2761.

Al-jabari, M., 2018. Numerical Simulation of Exchange Processes between Lagoons and the Red Sea in El Gouna , Egypt. Master Thesis, Water Engineering department, Technische Universität Berlin.

Authority, T.V., 1972. Heat and mass transfer between a water surface and the atmosphere. Tennessee Valley Authority, Division of Water Control Planning, Engineering ….

Bacon, J., Haverson, D., Devlin, M., Phillips, R., 2017. Modelling potential drivers of fish kill events in Sulaibikhat Bay, Kuwait, in: Proceedings of the XXIVth TELEMAC-MASCARET User Conference, 17 to 20 October 2017, Graz University of Technology, Austria. pp. 163–168.

Breitburg, D., Levin, L.A., Oschlies, A., Grégoire, M., Chavez, F.P., Conley, D.J., Garçon, V., Gilbert, D., Gutiérrez, D., Isensee, K., 2018. Declining oxygen in the global ocean and coastal waters. Science 359. https://doi.org/10.1126/science.aam7240

Cao, V., Schaffer, M., Taherdangkoo, R., Licha, T., 2020. Solute reactive tracers for hydrogeological applications: A short review and future prospects. Water (Switzerland) 12. https://doi.org/10.3390/w12030653

Cerralbo, P., Pedrera Balsells, M.F., Mestres, M., Fernandez, M., Espino, M., Grifoll, M., Sanchez-Arcilla, A., 2019. Use of a hydrodynamic model for the management of water renovation in a coastal system. Ocean Science 15, 215–226. https://doi.org/10.5194/os-15-215-2019

Chao, X., Jia, Y., Shields Jr, F.D., Wang, S.S.Y., Cooper, C.M., 2010. Three-dimensional numerical simulation of water quality and sediment-associated processes with application to a Mississippi Delta lake. Journal of environmental management 91, 1456–1466. https://doi.org/10.1016/j.jenvman.2010.02.009

Chapman, P.M., 2012. Management of coastal lagoons under climate change. Estuarine, Coastal and Shelf Science 110, 32–35. https://doi.org/10.1016/j.ecss.2012.01.010

Churchill, M.A., Elmore, H.L., Buckingham, R.A., 1964. the Prediction of Stream Reaeration Rates, in: Advances in Water Pollution Research, Proceedings of the International Conference Held in London. PERGAMON PRESS LTD, pp. 89–136. https://doi.org/10.1016/b978-1-4832-8391-3.50015-4

Danoun, R., 2007. Desalination Plants: Potential impacts of brine discharge on marine life. The Ocean Technology Group, the University of Sydney, Australia.

Diaz, R.J., Rosenberg, R., 1995. Marine benthic hypoxia: a review of its ecological effects and the behavioural responses of benthic macrofauna. Oceanography and marine biology. An annual review 33, 203–245.

Environmental, F., 2013. Dissolved Oxygen: Fundamentals of Environmental Measurements. Fondriest Environmental, Inc 19.

Fahmy, M.A., Fattah, L.M.A., Abdel-Halim, A.M., Aly-Eldeen, M.A., Abo-El-Khair, E.M., Ahdy, H.H., Ahdy, H.H., Hemeilly, A., El-Soud, A.A., Shreadah, M.A., 2016. Evaluation of the Quality for the Egyptian Red Sea Coastal Waters during 2011-2013. Journal of Environmental Protection 07, 1810–1834. https://doi.org/10.4236/jep.2016.712145

Flather, R.A., 1976. Results from a storm surge Prediction Model of the North European Contenental Shelf for April, November and December 1973. Technical Report 24, Wormley, UK, Institute of Oceanographic Sciences.

Fu, B., Merritt, W.S., Croke, B.F.W., Weber, T.R., Jakeman, A.J., 2019. A review of catchment-scale water quality and erosion models and a synthesis of future prospects. Environmental Modelling and Software 114, 75–97. https://doi.org/10.1016/j.envsoft.2018.12.008

Gattuso, J.P., Gentili, B., Duarte, C.M., Kleypas, J.A., Middelburg, J.J., Antoine, D., 2006. Light availability in the coastal

ocean: Impact on the distribution of benthic photosynthetic organisms and their contribution to primary production. Biogeosciences 3, 489–513. https://doi.org/10.5194/bg-3-489-2006

Gholizadeh, M.H., Melesse, A.M., Reddi, L., 2016. A comprehensive review on water quality parameters estimation using remote sensing techniques. Sensors (Switzerland) 16. https://doi.org/10.3390/s16081298

Gualtieri, C., Gualtieri, P., 1999. Statistical analysis of reaeration rate in streams, in: International Agricultural Engineering Conference (ICAE) Pechino, China, December 14–17.

Gurguess, S.M., Shreadah, M.A., Fahmy, M.A., Aboul El Kheir, E.M., Abdel Halim, A.M., 2009. Assessment of water quality in the Red Sea using in situ measurements and remote sensing data. Egyptian Journal of Aquatic Research 35, 1–13.

Haider, H., Ali, W., Haydar, S., 2013. Evaluation of various relationships of reaeration rate coefficient for modeling dissolved oxygen in a river with extreme flow variations in Pakistan. Hydrological Processes 27, 3949–3963. https://doi.org/10.1002/hyp.9528

Haurwitz, R., Broad, T., Collins, J., Carman, N., Arroyo, J., Krishna, H., Mannchen, B., McFadden, J., Stachowitz, A., 2008. DESALINATION: IS IT WORTH ITS SALT? A Primer on Brackish and Seawater Desalination.

Hervouet, J.-M., 2007. Hydrodynamics of free surface flows: modelling with the finite element method. Wiley Online Library, John Wiley, Chichester, U. K. https://doi.org/10.1002/9783527626250

Hervouet, J.M., Ata, R., 2017. Technical report: User manual of opensource software TELEMAC-2D V7P2, Report. EDF-R&D. www.opentelemac.org.

Holley, R.A., Liggett, T.M., 1975. Ergodic theorems for weakly interacting infinite systems and the voter model. The annals of probability 643–663.

Huang, J., Hu, J., Li, S., Wang, B., Xu, Y., Liang, B., Liu, D., 2019. Effects of physical forcing on summertime hypoxia and oxygen dynamics in the estuary. Water (Switzerland) 11. https://doi.org/10.3390/w11102080

Jahnke, C., Wannous, M., Troeger, U., Falk, M., Struck, U., 2019. Impact of seawater intrusion and disposal of desalinization brines on groundwater quality in El Gouna, Egypt, Red Sea Area. Process analyses by means of chemical and isotopic signatures. Applied Geochemistry 100, 64–76. https://doi.org/10.1016/j.apgeochem.2018.11.00

Jones, E., Qadir, M., van Vliet, M.T.H., Smakhtin, V., Kang, S. mu, 2019. The state of desalination and brine production: A global outlook. Science of the Total Environment 657, 1343–1356. https://doi.org/10.1016/j.scitotenv.2018.12.076

Kennish, M.J., Paerl, H.W., 2010. Coastal lagoons: critical habitats of environmental change. CRC Marine Science Series. CRC Press, Boca Raton.

Kinzelbach, W., 1992. Numerische Methoden zur Modellierung des Transports von Schadstoffen im Grundwasser. Oldenbourg.

Lattemann, S., Höpner, T., 2008. Environmental impact and impact assessment of seawater desalination. Desalination 220, 1–15. https://doi.org/10.1016/j.desal.2007.03.009

Lee, Y.W., Park, M.O., Kim, S.G., Kim, S.S., Khang, B., Choi, J., Lee, D., Lee, S.H., 2021. Major controlling factors affecting spatiotemporal variation in the dissolved oxygen concentration in the eutrophic Masan Bay of Korea. Regional Studies in Marine Science 46, 101908. https://doi.org/10.1016/j.rsma.2021.101908

Mahaffey, C., Palmer, M., Greenwood, N., Sharples, J., 2020. Impacts of climate change on dissolved oxygen concentration relevant to the coastal and marine environment around the UK. MCCIP Science Review 2020, 31–53. https://doi.org/10.14465/2020.arc02.oxy

Marlina, N., Melyta, D., 2019. Analysis Effect of Cloud Cover, Wind Speed, and Water Temperature to BOD and DO Concentration Using QUAL2Kw Model (Case Study In Winongo River, Yogyakarta). MATEC Web of Conferences 280, 05006. https://doi.org/10.1051/matecconf/201928005006

Newton, A., Brito, A.C., Icely, J.D., Derolez, V., Clara, I., Angus, S., Schernewski, G., Inácio, M., Lillebø, A.I., Sousa, A.I., Béjaoui, B., Solidoro, C., Tosic, M., Cañedo-Argüelles, M., Yamamuro, M., Reizopoulou, S., Tseng, H.C., Canu, D., Roselli, L., Maanan, M., Cristina, S., Ruiz-Fernández, A.C., Lima, R.F. d., Kjerfve, B., Rubio-Cisneros, N., Pérez-Ruzafa, A., Marcos, C., Pastres, R., Pranovi, F., Snoussi, M., Turpie, J., Tuchkovenko, Y., Dyack, B., Brookes, J., Povilanskas, R., Khokhlov, V., 2018. Assessing, quantifying and valuing the ecosystem services of coastal

lagoons. Journal for Nature Conservation 44, 50–65. https://doi.org/10.1016/j.jnc.2018.02.009

Ni, X., Huang, D., Zeng, D., Zhang, T., Li, H., Chen, J., 2016. The impact of wind mixing on the variation of bottom dissolved oxygen off the Changjiang Estuary during summer. Journal of Marine Systems 154, 122–130. https://doi.org/10.1016/j.jmarsys.2014.11.010

O'Connor, D.J., Dobbins, W.E., 1958. Mechanism of reaeration in natural streams. Transactions of the American Society of Civil Engineers 123, 641–666.

Owens, S. de la P., Innis, S.M., 1999. Docosahexaenoic and arachidonic acid prevent a decrease in dopaminergic and serotoninergic neurotransmitters in frontal cortex caused by a linoleic and α-linolenic acid deficient diet in formula-fed piglets. The Journal of nutrition 129, 2088–2093. https://doi.org/10.1093/jn/129.11.2088

Panda, U.S., Mahanty, M.M., Ranga Rao, V., Patra, S., Mishra, P., 2015. Hydrodynamics and water quality in Chilika Lagoon-A modelling approach. Procedia Engineering 116, 639–646. https://doi.org/10.1016/j.proeng.2015.08.337

Pastore, D.M., Peterson, R.N., Fribance, D.B., Viso, R., Hackett, E.E., 2019. Hydrodynamic drivers of dissolved oxygen variability within a tidal creek in Myrtle Beach, South Carolina. Water (Switzerland) 11. https://doi.org/10.3390/w11081723

Pérez-Ruzafa, A., Campillo, S., Fernández-Palacios, J.M., García-Lacunza, A., García-Oliva, M., Ibañez, H., Navarro-Martínez, P.C., Pérez-Marcos, M., Pérez-Ruzafa, I.M., Quispe-Becerra, J.I., Sala-Mirete, A., Sánchez, O., Marcos, C., 2019. Long-term dynamic in nutrients, chlorophyll a, and water quality parameters in a coastal lagoon during a process of eutrophication for decades, a sudden break and a relatively rapid recovery. Frontiers in Marine Science 6, 1–23. https://doi.org/10.3389/fmars.2019.00026

Rasul, N.M.A., Stewart, I.C.F., Vine, P., Nawab, Z.A., 2019. Introduction to oceanographic and biological aspects of the Red Sea, in: Oceanographic and Biological Aspects of the Red Sea. Springer,Cham., pp. 1–9. https://doi.org/10.1007/978-3-319-99417-8_1

Richardson, J.L., Arndt, J.L., Montgomery, J.A., 2001. Hydrology of wetland and related soils. Wetland soils–Genesis, hydrology, landscapes, and classification 35–84.

Seiler, L.M.N., Fernandes, E.H.L., Siegle, E., 2020. Effect of wind and river discharge on water quality indicators of a coastal lagoon. Regional Studies in Marine Science 40, 101513. https://doi.org/10.1016/j.rsma.2020.101513

Shamsudin, S.N., Azman, A.A., Ismail, N., Rahiman, M.H.F., Ahmad, A.H., Taib, M.N., 2016. Review on significant parameters in water quality and the related artificial intelligent applications. Proceedings - 2015 6th IEEE Control and System Graduate Research Colloquium, ICSGRC 2015 163–168. https://doi.org/10.1109/ICSGRC.2015.7412485

Talley, L., 2000. Properties of seawater (lecture 2). SIO: Introduction to Physical Oceanography. http://talleylab. ucsd. edu/ltalley/sio210/oct1/index. html.

Thomann, R. V, Mueller, J.A., 1987. Principles of surface water quality modeling and control. Harper & Row Publishers.

Tularam, G.A., Ilahee, M., 2007. Environmental concerns of desalinating seawater using reverse osmosis. Journal of Environmental Monitoring 9, 805–813. https://doi.org/10.1039/b708455m

User manual of opensource software TELEMAC-2D V7P2, 2017. TELEMAC-2D Software.

Van Genuchten, M.T., Leij, F.J., Skaggs, T.H., Toride, N., Bradford, S.A., Pontedeiro, E.M., 2013. Exact analytical solutions for contaminant transport in rivers 1. The equilibrium advection-dispersion equation. Journal of Hydrology and Hydromechanics 61, 146–160. https://doi.org/10.2478/johh-2013-0020

Venkiteswaran, J.J., Wassenaar, L.I., Schiff, S.L., 2007. Dynamics of dissolved oxygen isotopic ratios: A transient model to quantify primary production, community respiration, and air-water exchange in aquatic ecosystems. Oecologia 153, 385–398. https://doi.org/10.1007/s00442-007-0744-9

Watt, M.K., 2000. A hydrologic primer for New Jersey watershed management. US Department of the Interior, US Geological Survey.

Wetzel, R.G., 2001. Limnology: lake and river ecosystems. gulf professional publishing.

Appendix A

A1 Theoretical aspects of flow and transport equations

The flow governing equations are the continuity equation, the momentum equations in both x- and y-direction and the tracer transport equation:

$$\frac{\partial \mathrm{h}}{\partial \mathrm{t}} + \vec{\mathrm{u}} * \mathrm{grad\ h} + \mathrm{h div}\,\vec{\mathrm{u}} = S_h \tag{1}$$

$$\frac{\partial u}{\partial \mathrm{t}} + \vec{u}\,\mathrm{grad\ u} = -\mathrm{g}\frac{\partial Z}{\partial \mathrm{x}} + S_x + \frac{1}{\mathrm{h}}\,\mathrm{div}\left(h_{v_t}\,\mathrm{grad\ u}\right) \tag{2}$$

$$\frac{\partial v}{\partial \mathrm{t}} + \vec{u} * \mathrm{grad\ v} = -\mathrm{g}\frac{\partial Z}{\partial \mathrm{y}} + S_y + \frac{1}{\mathrm{h}}\mathrm{div}\left(h_{v_t}\,\mathrm{grad\ v}\right) \tag{3}$$

$$\frac{\partial \mathrm{C}}{\partial \mathrm{t}} + \vec{u} * \mathrm{grad\ C} = F_i + \frac{1}{\mathrm{h}}\mathrm{div}\left(h_{v_T}\,\mathrm{grad\ C}\right) \tag{4}$$

Where h is the water depth (m), C is the tracer (g/l), u, v are velocities in x- and y-directions (m/s), g is the acceleration of gravity, v_t, v_T is the turbulent viscosity and turbulent diffusivity, Z is the free surface elevation (m), t is time (s), x, y are horizontal space coordinates (m), S_h, F_i are the sources or sinks of fluid (m/s) and tracer (g/l/s) and S_x, S_y are source or sink terms in momentum equations (m/s^2).

One of the most important sink terms of momentum is the bed friction. Several formulas exist to calculate the bottom friction (Hervouet, 2007). In this work, the bottom friction followed Strickler's law in both x and y direction as:

$$f_x = -\frac{g}{k_{st}^2 h^{\frac{1}{3}}}\frac{\rho}{h}u\sqrt{u^2+v^2} \tag{5}$$

$$f_y = -\frac{g}{k_{st}^2 h^{\frac{1}{3}}}\frac{\rho}{h}v\sqrt{u^2+v^2} \tag{6}$$

Where k_{St} is the Strickler's coefficient and ρ is the density of water (kg/m^3).

Flather's approach (Flather, 1976) is adopted in TELEMAC-2D for calculating the wind shear stress. The governing equations of the wind simulation and the different formulas for determining coefficient a_{wind} are reported in equations (7), (8) and (9):

$$S_x = \frac{1}{h}\frac{\rho_{air}}{\rho_{water}}a_{wind}u_{wind}\sqrt{u_{wind}^2+v_{wind}^2} \tag{7}$$

$$S_y = \frac{1}{h}\frac{\rho_{air}}{\rho_{water}}a_{wind}v_{wind}\sqrt{u_{wind}^2+v_{wind}^2} \tag{8}$$

$$\begin{aligned}&\text{if } \|u_{wind}\| \le 5\,{}^{m}/_{s}, a_{wind} = 0.565 * 10^{-3}\\ &\text{if } 5\,{}^{m}/_{s} < \|u_{wind}\| < 19.2\,{}^{m}/_{s}, a_{wind} = (-0.12 + 0.137\,\|u_{wind}\|) * 10^{-3}\\ &\text{if } \|u_{wind}\| > 19.2\,{}^{m}/_{s}, a_{wind} = 2.513 * 10^{-3}\end{aligned} \tag{9}$$

Where u_{wind}, v_{wind} are wind velocity components at 10 m height, ρ_{air} is the density of air, a_{wind} is the wind shear stress coefficient, which in turn depends on the value of wind velocity.

A2 Analytical solutions

The tracer's transport equations for DO in 1D flow for both the pulse (equation 11) and constant injection (equation 12) of DO are analytically applied according to Kinzelbach (1992) as follows:

$$\frac{\partial O_2}{\partial t} + \frac{u}{R}\frac{\partial O_2}{\partial x} = \frac{D_L}{R}\frac{\partial^2 O_2}{\partial x^2} - \lambda_{o_2} \quad (10)$$

$$O_{2,\delta}(x,t) = \frac{\Delta M}{2n_e mBR\sqrt{\alpha_L}\sqrt{\frac{\pi ut}{R}}} e^{-\frac{\left(x-\frac{ut}{R}\right)^2}{4\alpha_L\frac{ut}{R}}} e^{-\lambda_{o_2}t} \quad (11)$$

$$O_2(x,t) = \frac{O_{2,0}}{2} e^{\frac{x}{2\alpha_L}} \left[e^{\frac{-x\gamma}{2\alpha_L}} * erfc\left(\frac{x-\frac{ut\gamma}{R}}{2\sqrt{\frac{\alpha_L ut}{R}}}\right) - e^{\frac{x\gamma}{2\alpha_L}} * erfc\left(\frac{x+\frac{ut\gamma}{R}}{2\sqrt{\frac{\alpha_L ut}{R}}}\right)\right] \quad (12)$$

Where u is the flow velocity in 1D (m/s), D_L is longitudinal dispersion coefficient (m^2/s), R is retardation factor (-), λ_{o_2} is degradation of DO (s^{-1}), ΔM is DO mass at instantaneous addition rate (mg), n_e is effective porosity (=1 for water), m is saturated flow thickness (m), B is flow width (m), α_L is longitudinal dispersity, which equals (D_L/u) (m) and δ is delta function (1/m), $O_{2,0}$ is the initial distribution of DO concentration (mg/m^3)

The 2D tracer transport equation for DO in horizontal flow for constant injection of DO is analytically determined according to Kinzelbach (1992) (Kinzelbach, 1992) as follows:

$$O_2(x,y,t) = \frac{\dot{M}}{4n_e mu\sqrt{\pi\alpha_T}} e^{\frac{x-r\gamma}{2\alpha_L}} \frac{1}{\sqrt{r\gamma}} erfc\left(\frac{r-\frac{ut\gamma}{R}}{2\sqrt{\alpha_L u\frac{t}{R}}}\right) \quad (13)$$

$$r = \sqrt{x^2 + \frac{\alpha_L}{\alpha_T}y^2}, \gamma = \sqrt{1 + 4\alpha_L\lambda_{o_2}\frac{R}{u}} \quad (14)$$

Where α_T is the transversal dispersity (m) and is assumed to equal α_L.

A3 TELEMAC-WAQTEL- O_2 model

The oxygen concentration is varying under the influence of sources with respect to the following law:

$$F[O_2] = K_2(C_s - [O_2]) - K_1[L] - K_4[NH_4] + P - R - \frac{BEN}{h} \quad (15)$$

In the TELEMAC-WAQTEL-O_2 model, four formulas can be chosen for calculating the reaeration coefficient:

Formula of Tenessee Valley Authority (Authority, 1972): $K_2 = 5.23\, u\, h^{-1.67}$ (16)

Formula of Owens et al. (Owens and Innis, 1999): $K_2 = 5.33\, u^{0.67} h^{-1.85}$ (17)

Formula of Churchill et al. (Churchill et al., 1964): $K_2 = 0.746\, u^{2.695} h^{-3.085} J^{-0.823}$ (18)

Formula of O'Connor & Dobbins (O'Connor and Dobbins, 1958): $K_2 = 3.9 u^{0.5} h^{-1.5}$ (19)

Where J is head loss (-)

A final formula combines the three last formulas being also available in TELEMAC-WAQTEL-O_2 model, where choosing the K_2 formula depends on the water depth and velocity at each point of the mesh (User manual of opensource software TELEMAC-2D V7P2, 2017):

$K_2 = 5.23\, u^{0.67} h^{-1.85}$ if $h < 0.6$

$K_2 = 0.746\, u^{2.695} h^{-3.085} J^{-0.823}$ if $0.6 < h < 15, 0.6 < u < 1.9$

$K_2 = 3.9u^{0.5}h^{-1.5}$ elsewhere (20)

For the aforementioned formulas, the calculated reaeration coefficient is determined at $20°C$. Correction of the temperature variation is computed as:

$(K_2)_T = (K_2)_{20}(\theta^{T-20})$ (21)

Further, the oxygen saturation concentration of water (C_s) is mainly dependent on the temperature. TELEMAC-WAQTEL offers the two most common formulas to calculate C_s:

Formula of Elmore & Hayes: $C_s = 14.652 - 0.41022T + 0.00799T^2 - 7.7774.10 - 5T^3$ (22)

Formula of Montgomery (Richardson et al., 2001): $C_s = 468/(31.6+T)$ (23)

The following table illustrates input parameters for production and consumption of DO in TELEMAC-WAQTE-O_2 model, their reference values and the effect of water temperature.

Parameter	Value	Temperature effect	Process
Benthic demand (BEN_T)	Depends on bed type: • filamentous bacteria (10 g/m2) =7gDO/m^2/d • mud from wastewater, near to release = 4 gDO/m^2/d • mud from wastewater far from release = 1.5 gDO/m^2/d • estuarine silt = 1.5 gDO/m^2/d Sand = 0.5 gDO/m^2/d • mineral soil = 0.007 gDO/m^2/d	$BEN_T = BENT_{20°}(1.065)^{T-20}$	Consumption
Vegetal respiration(R)	Default value of 0.06 mgDO/d/l		Consumption
Photosynthesis (P)	Ranges from 0.3 to 9 mgDO/d/l (depends on sunlight, depth and algae density)		production
Reaeration coefficient (K_2)	Ranges from 0.1 d^{-1} to more than 1.15 d^{-1} depending on the water type and is calculated from formulas depending on water depth and flow velocity (equation 16,17,18,19,20)	$(K_2)_T = (K_2)_{20}(\theta^{T-20})$	production
The oxygen density at saturation (C_S)	Can be calculated using two formulas depending on the water temperature (equation 22 and 23)	$C_s = 14.652 - 0.41022T + 0.00799T^2 - 7.7774.10 - 5T^3$ $C_s = 468/(31.6+T)$	production
The kinetic organic load (K_1)	0.25 d^{-1}		Consumption
Constant of nitrification (K_4)	0.35 d^{-1}		Consumption

Figures caption

Fig. 1: Location of the study area in Egypt: (a) El Gouna city, (b) capture of El Gouna lagoons (adapted by the author from Google Earth (2020) and (c) computational domain showing observation points, water depth (m), inflow and outflow boundaries (red circles: open boundaries to neighboring lagoons, blue circle: open boundary to desalination plant) and zoom of the unstructured triangular mesh.

Fig. 2: DO concentrations in simple domain with stagnant water for four simulation days (96 hr) in two different cases: the effect of reaeration coefficient only (case 1) and the effect of both reaeration coefficient and saturation density (case 2)

Fig. 3: Comparison between DO concentrations (mg/l) for the analytical and simulation results in the whole domain for different time steps under the effect of a) pulse injection of DO and b) constant injection of DO

Fig. 4: Results of selected points at different distances from X-axis for the whole calculation period of 4 days (345600 s) using both calculation methods.

Fig. 5: comparison between saturation DO concentrations and the average simulated DO for 4 days using TELEMAC-WAQTEL-O_2 model at different water temperatures

Fig. 6: DO concentrations in El Gouna lagoons after 8 simulation days a) DO-TEMP20 , b) DO-TEMP30

Fig. 7: DO concentrations (mgDO/l) at observation points over the 8 days of simulation considering DO-TIDE-MW

Fig. 8: DO concentrations (mgDO/l) at control points over 8 days of simulation considering DO-TIDE scenario

Fig. 9: DO concentrations (mgDO/l) after 8 days of simulation considering DO-MW scenario

Fig. 10: DO concentrations (mgDO/l) at control points over 8 days of simulation considering DO-MW scenario

Fig. 11: DO concentrations (mgDO/l) after 8 days of simulation considering DO-MAXW scenario

Fig. 12: DO concentrations (mgDO/l) at control points over 8 days of simulation considering DO-MAXW scenario

Fig. 13: DO concentrations (mgDO/l) at four control points over 8 days of simulation considering the effect of binary discharge (BRI-ZERO and BRI-DO3 scenarios)

Fig. 14: Propagation of polluted binary discharge with low DO concentration in the lagoons after 5 days of simulation in case of a) BRI-TIDE, b) BRI-MW and c) BRI-MAXW

Figures

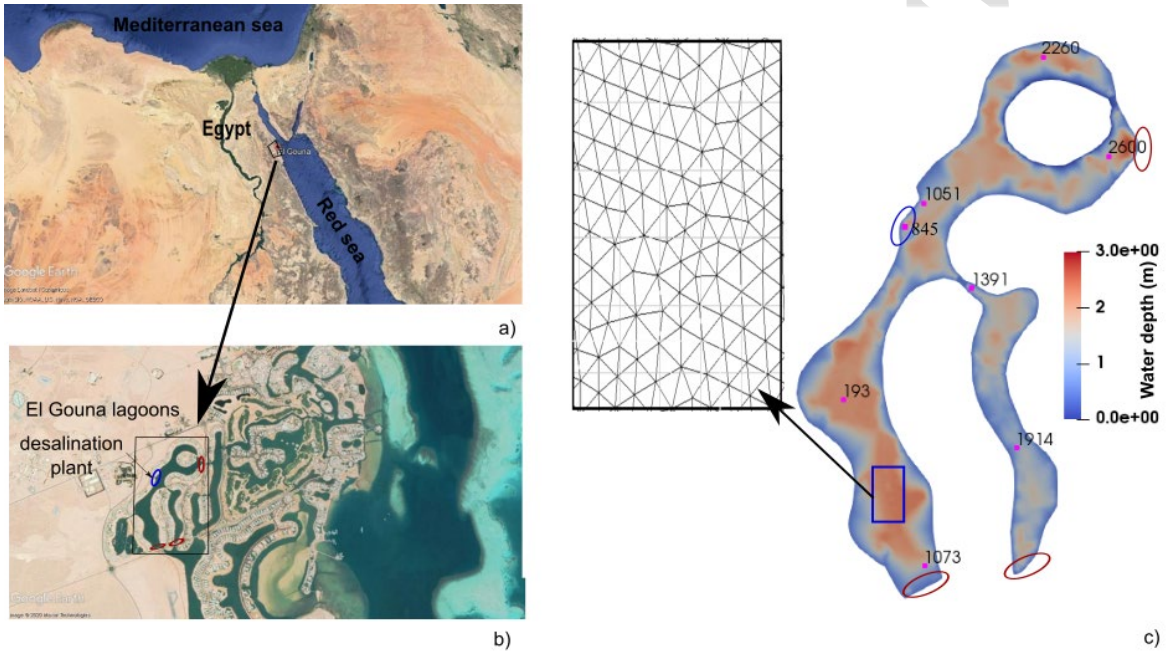

Fig. 1: Location of the study area in Egypt: (a) El Gouna city, (b) capture of El Gouna lagoons (adapted by the author from Google Earth (2020) and (c) computational domain showing observation points, water depth (m), inflow and outflow boundaries (red circles: open boundaries to neighboring lagoons, blue circle: open boundary to desalination plant) and zoom of the unstructured triangular mesh.

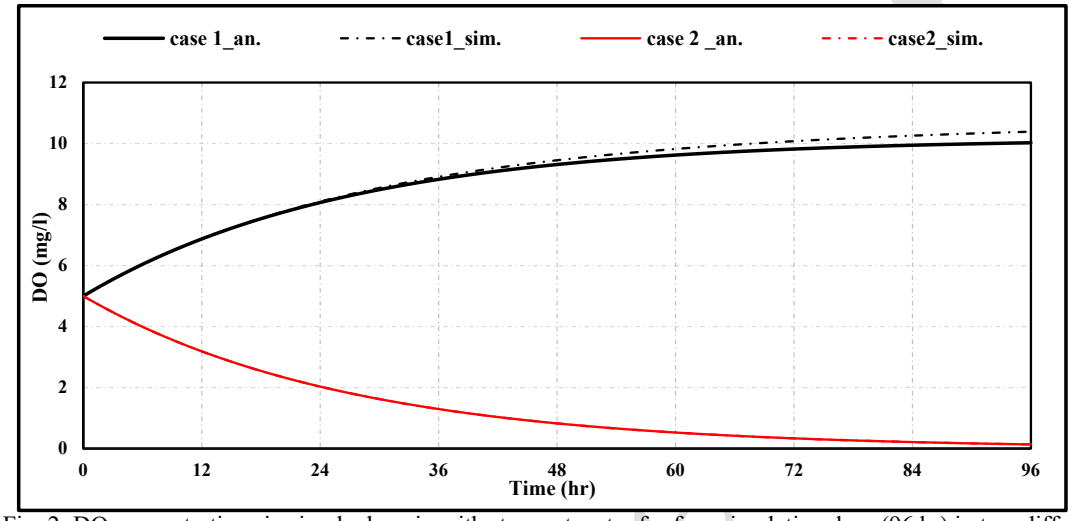

Fig. 2: DO concentrations in simple domain with stagnant water for four simulation days (96 hr) in two different cases: the effect of reaeration coefficient only (case 1) and the effect of both reaeration coefficient and saturation density (case 2)

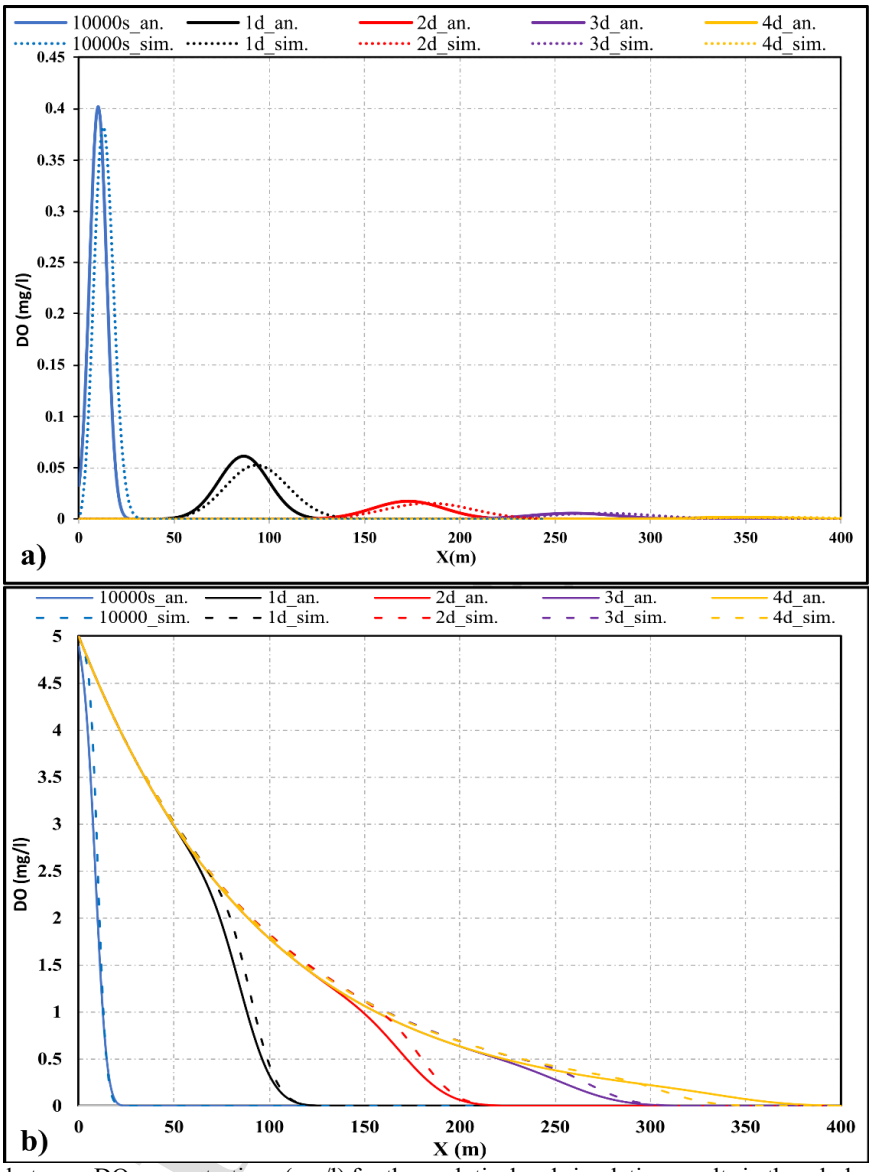

Fig. 3: Comparison between DO concentrations (mg/l) for the analytical and simulation results in the whole domain for different time steps under the effect of a) pulse injection of DO and b) constant injection of DO.

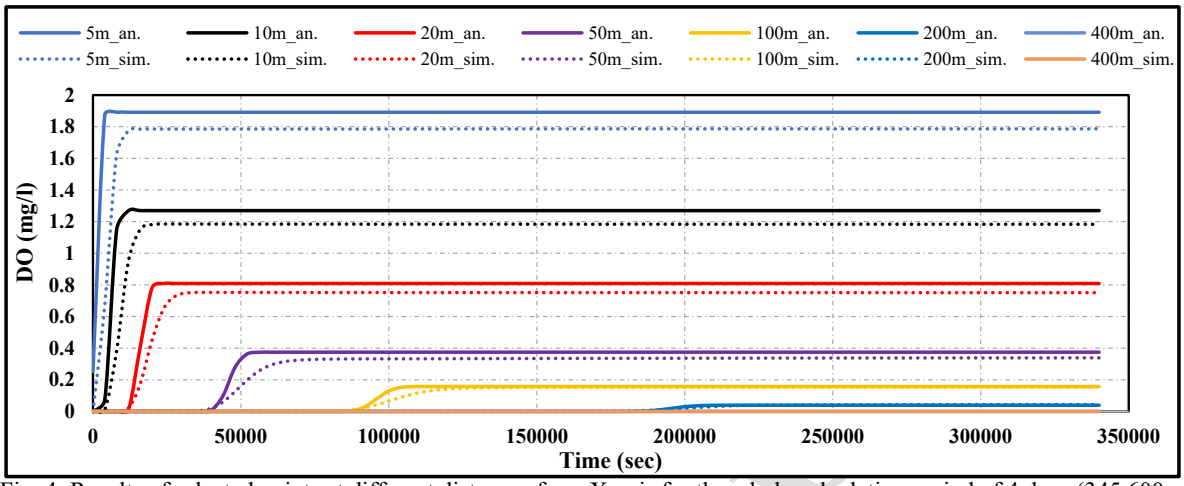

Fig. 4: Results of selected points at different distances from X-axis for the whole calculation period of 4 days (345,600 s) using both calculation methods.

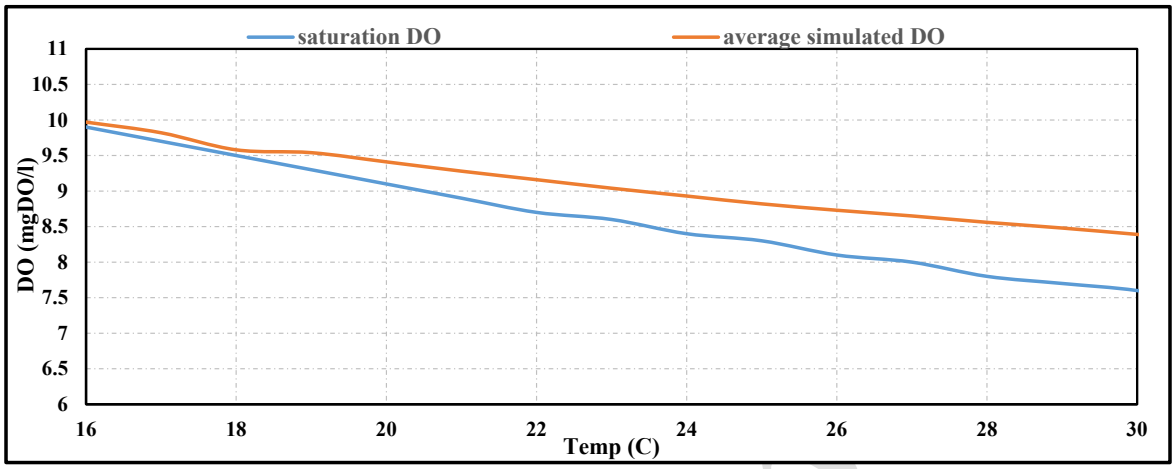

Fig. 5: Comparison between saturation DO concentrations and average simulated DO for 8 days using TELEMAC-WAQTEL-O_2 model at different water temperatures.

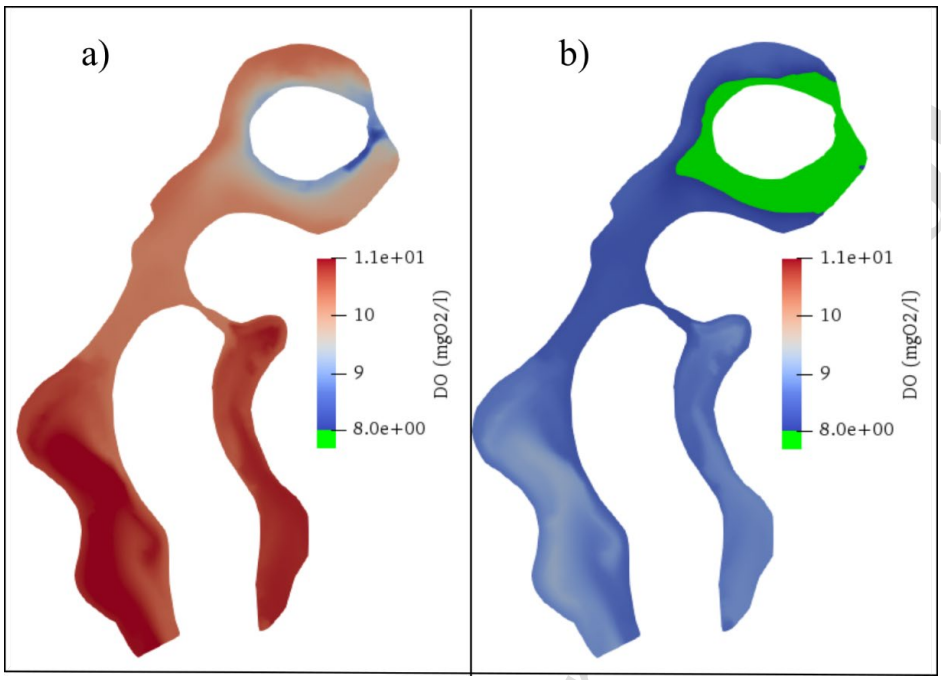

Fig. 6: DO concentrations in El Gouna lagoons after 8 simulation days a) DO-TEMP20 , b) DO-TEMP30

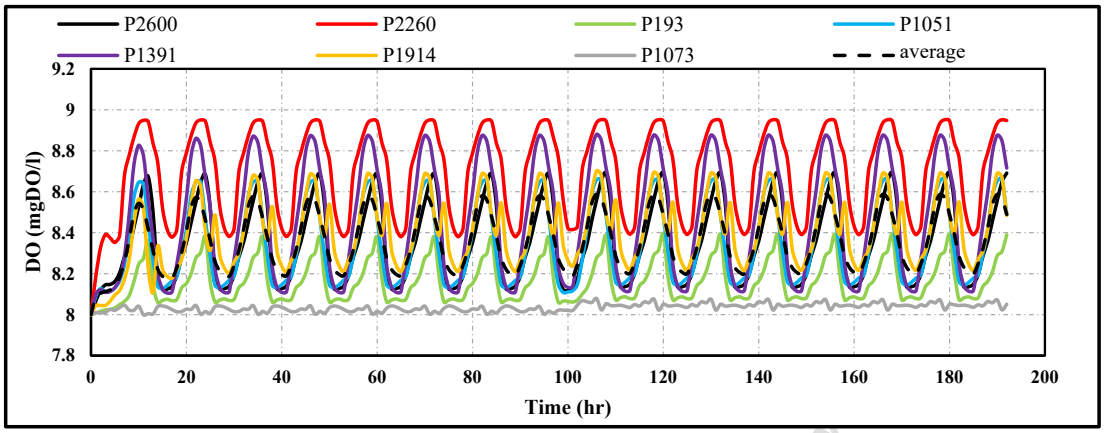

Fig. 7: DO concentrations (mgDO/l) at observation points over the 8 days of simulation under the effect of tide with mean wind

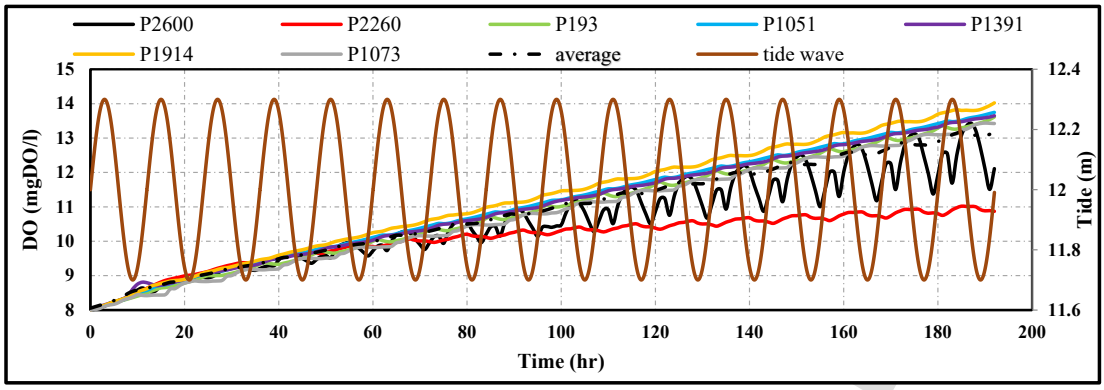

Fig. 8: DO concentrations (mgDO/l) at control points over 8 days of simulation considering DO-TIDE scenario

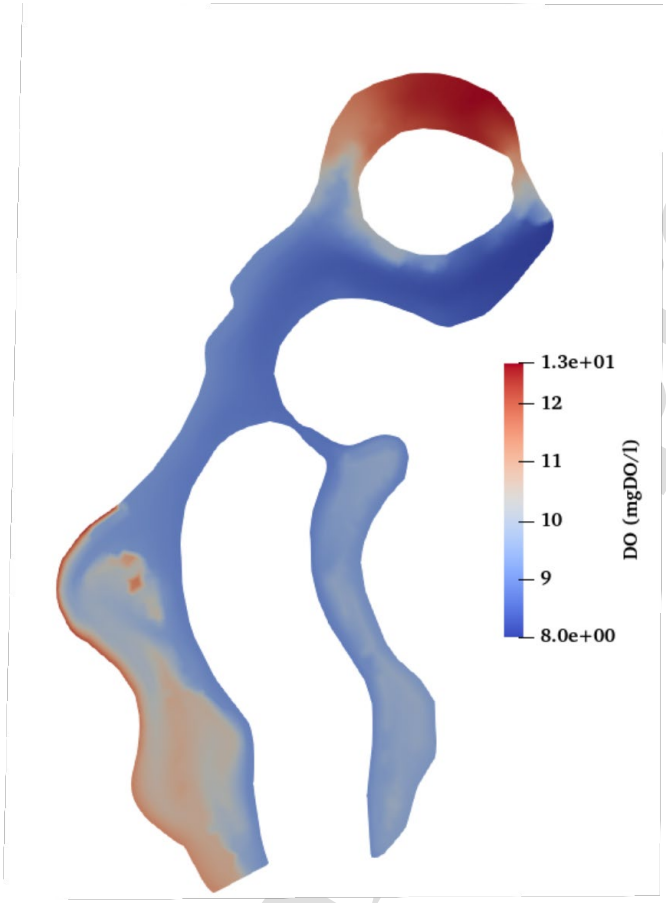

Fig. 9: DO concentrations (mgDO/l) after 8 days of simulation considering DO-MW scenario

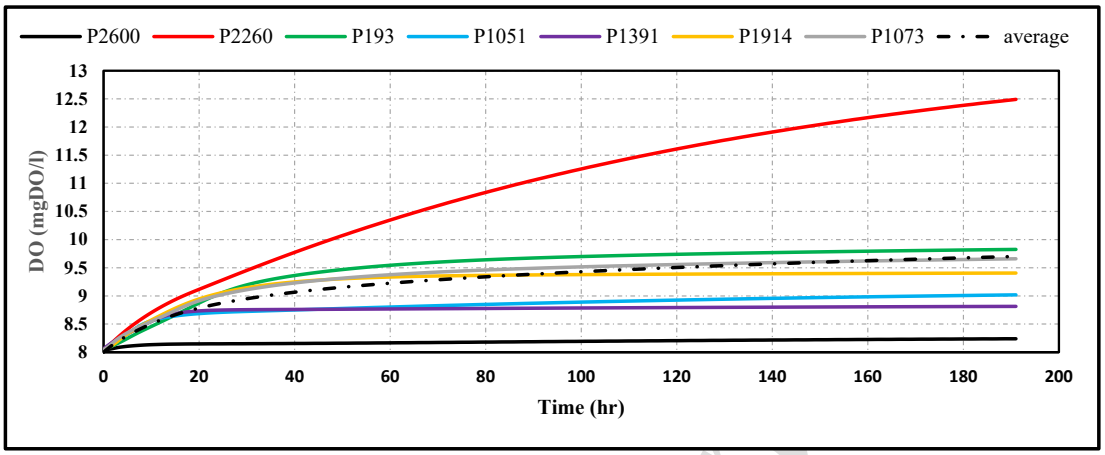

Fig. 10: DO concentrations (mgDO/l) at control points over 8 days of simulation considering DO-MW scenario

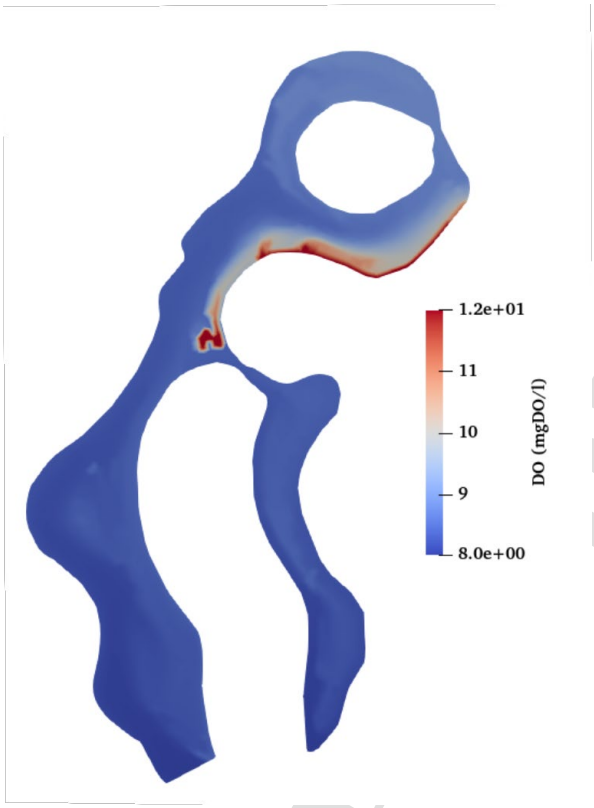

Fig. 11: DO concentrations (mgDO/l) after 8 days of simulation considering DO-MAXW scenario

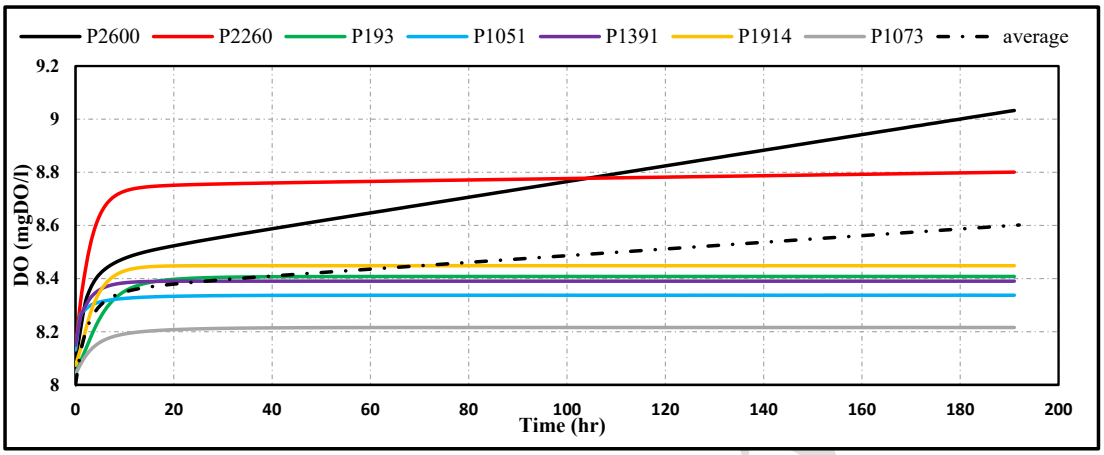

Fig. 12: DO concentrations (mgO_2/l) at control points over 8 days of simulation considering DO-MAXW scenario

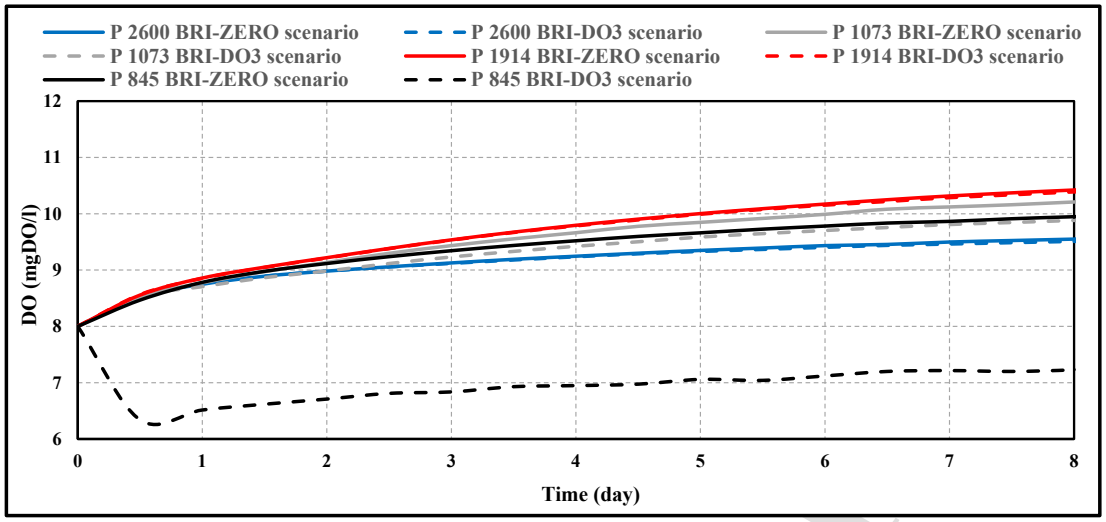

Fig. 13: DO concentrations (mgO_2/l) at four control points over 8 days of simulation considering the effect of binary discharge (BRI-ZERO and BRI-DO3 scenarios)

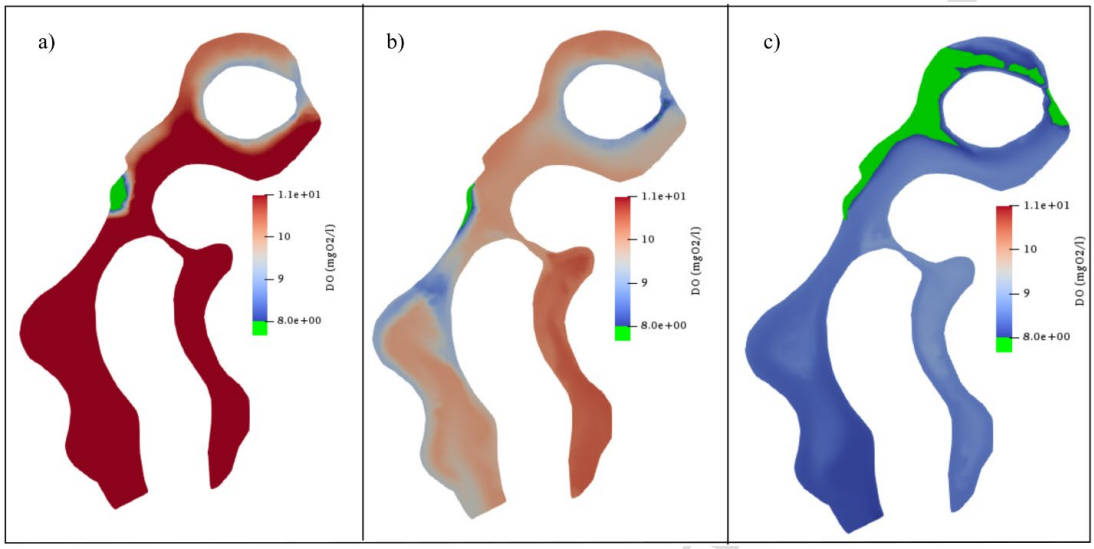

Fig. 14: Propagation of polluted binary discharge with low DO concentration in the lagoons after 5 days of simulation in case of a) BRI-TIDE, b) BRI-MW and c) BRI-MAXW

Highlights

Agreement between TELEMAC-WAQTEL-O_2 model and analytical solution in 1D and 2D

Dissolved oxygen decreased when water temperature increased

Tide created a sinusoidal dissolved oxygen wave inversely proportional to water depths

Water inflow area presented low dissolved oxygen compared to high outflow values

Quantity of binary and different injection time had minor effects on dissolved oxygen

Credit Author statement:

Omnia Abouelsaad: Conceptualization, Methodology, Investigation, Software, Writing – Original draft

Elena Matta: Investigation, Co-supervision, Writing-Review & Editing

Mohie ElDin M. Omar: Investigation, Writing-Review & Editing

Reinhard Hinkelmann: Conceptualization, Supervision, Writing-Review & Editing

Declaration of interests

☐ The authors declare that they have no known competing financial interests or personal relationships that could have appeared to influence the work reported in this paper.

☒ The authors declare the following financial interests/personal relationships which may be considered as potential competing interests:

Omnia Abouelsaad reports financial support was provided by Cultural Affairs and Missions Sector, Ministry of Higher Education in Egypt.